PPS Perspective
www.rsc.org/pps

Time-resolved photothermal methods: accessing time-resolved thermodynamics of photoinduced processes in chemistry and biology †

Thomas Gensch [a] **and Cristiano Viappiani** [b]

[a] *Forschungszentrum Jülich, Institut für Biologische Informationsverarbeitung 1, 52425 Jülich, Germany. E-mail: t.gensch@fz-juelich.de*
[b] *Dipartimento di Fisica, Università di Parma, Istituto Nazionale per la Fisica della Materia (INFM), Parco Area delle Scienze 7A, 43100 Parma, Italy. E-mail: cristiano.viappiani@fis.unipr.it*

Received 21st March 2003, Accepted 13th May 2003
First published as an Advance Article on the web 12th June 2003

Photothermal methods are currently being employed in a variety of research areas, ranging from materials science to environmental monitoring. Despite the common term which they are collected under, the implementations of these techniques are as diverse as the fields of application. In this review, we concentrate on the recent applications of time-resolved methods in photochemistry and photobiology.

1 Introduction

When photothermal methods entered the fields of photobiology and photochemistry, they were an issue to be studied in themselves, since their potential and meaning were largely to be determined and their reliability was also under scrutiny.

While new methods and applications based on photothermal effects are still being pursued, the emphasis of current work is more on the quality of the information that can be retrieved from the experiments. More than 20 years after the first pioneering studies in this field,[1–4] photothermal methods are now being reliably used to quantitate thermodynamic parameters and rate constants of light-initiated reactions—by direct photoreactions or by light-induced environmental changes (*e.g.* pH jump)—with kinetics spanning over a broad time range, extending from the picoseconds to several milliseconds.[5–9] These parameters are simply not obtainable by using other spectroscopic methods and, in this respect, photothermal methods are essential for complete understanding of the mechanisms and energy redistribution among reaction steps of photoinduced processes.

† Dedicated to Professor Silvia Braslavsky, to mark her great contribution to photochemistry and photobiology particularly in the field of photothermal methods.

Thomas Gensch was born in 1966 in Berlin, Germany. He graduated in Physics at the Humboldt University, Berlin, in 1992 and did his PhD (Photoacoustic Spectroscopy of Biological Photoreceptors, 1996) at the Max Planck Institute of Radiation Chemistry, Mülheim an der Ruhr, Germany. As a postdoc at the Katholieke Universiteit Leuven, Belgium, he worked on fluorescence microscopy, spectroscopy and optical tweezers (1997–1999). Thomas won the Casimir–Ziegler Award (1998), which allowed him to become a postdoc at the University of Amsterdam, Netherlands, working on the photoreceptor PYP. Since August 2000, he has been at the Research Center Jülich (IBI-1). His research interests include biological photoreceptors, autofluorescent proteins, fluorescence microscopy and spectroscopy, and protein folding.

Thomas Gensch

Cristiano Viappiani is Professor of Applied Physics at the Faculty of Pharmacy of the University of Parma, Italy, where he received his PhD in Physics. His research activity is mainly concerned with the use of nanosecond laser-based techniques, including time-resolved photoacoustics, to investigate protein structural dynamics and function. He has recently introduced laser-induced pH-jump techniques to the field of protein folding and is actively working on the development and photochemical characterization of photolabile caged compounds. His interests include the dynamics of immobilized proteins using laser flash photolysis.

Cristiano Viappiani

DOI: 10.1039/b303177b

A particularly fascinating development has been the use of photothermal methods to determine time-resolved volume changes during photoinitiated reactions,[1] which allows us to "hear" proteins moving during their functions on the picosecond to millisecond timescales.[5,8,9] The challenge is now to relate the measured parameters (Fig. 1) to fundamental physical and chemical quantities, and to interpret them at the molecular level.[10–12]

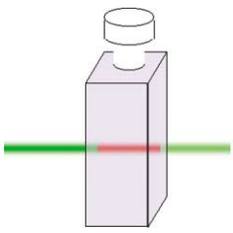

Fig. 1 The main sources of the photothermal effects and the corresponding parameters monitored in photothermal methods. The symbols used are defined as follows: T, temperature; V, volume; P, pressure; H, enthalpy; S, entropy; ρ, mass density; n, refractive index; c, molar concentration; A, absorbance.

Photothermal methods are a group of high sensitivity methods which were originally developed, and still are widely used, to measure optical absorption,[3] but with the potential of giving access to a variety of thermodynamic and kinetic parameters for the events induced in a sample by absorption of light. The basis of the collective term *photothermal* for these techniques comes from the detection of *thermal* relaxation of excess energy associated with *photo*excitation of the sample. It must be said that this terminology, although respectful of the historical background, is probably not completely correct, since many of the effects detected in modern photobiological and photochemical applications are not of thermal origin.[5,9] Volume changes are at the basis of the pressure wave detected in time-resolved photoacoustics, and these volume changes can be either thermal or non-thermal in origin. Photothermal lensing, beam deflection, and grating techniques detect changes in refractive index arising from changes in density (resulting from a change in volume of either thermal or structural origin), in absorbance (through the Kramers–Kronig relation), and in temperature. When light energy is absorbed and subsequently dissipated as heat without any other effects (structural volume and refractive index changes due to transient absorbance), it results in sample heating. This heating leads to a temperature change as well as changes in the thermodynamic parameters of the sample which are related to temperature. Measurement of the temperature, pressure, or density changes that occur due to optical absorption are ultimately the basis for all photothermal spectroscopic methods. The existence of signals of non-thermal origin superimposed on those originating from enthalpic changes is a possible source of complexity in the data analysis. However, instead of being a drawback, this has turned out to be a unique feature of the methods, which can, in principle, yield a wealth of information otherwise not obtainable. The price to pay is that data analysis in modern experiments is often more complicated than it used to be at the early developmental stages of the techniques, and in many cases requires sophisticated approaches. However, in a number of situations of practical interest, the data analysis can be simplified by making reasonable assumptions. Volume changes of non-thermal origin may reflect several possible effects, such as changes in the number of charges in solution, changes in the dipole moment of the solutes, changes in the interaction between solute and solvent molecules, and changes in the molarity of a particular component, amongst others. In the following, we will refer to these volume changes as structural volume changes, regardless of the specific mechanism which underlies them. The magnitude of the molecular volume changes and their involvement in signal generation are expected to be relevant for photoinduced reactions involving a change in the number of reactants and product molecules, or large changes in charge distributions between reactants and products.[13–15] It is in these cases that the structural contributions must be taken into account when calculating enthalpic changes, which otherwise will be affected by systematic errors. An example is the use of a water-soluble porphyrin as a standard in photoacoustic spectroscopy, where the structural volume change upon triplet generation[16] was neglected.[17]

The photothermal methods with high temporal resolution that have been developed so far are mainly suitable for studies on liquid samples, but the transient grating and lensing techniques are, in principle, applicable to optically transparent, solid samples. We can divide the photothermal methods into two main classes according to the parameter being monitored: photoacoustic methods are based on the detection of the pressure wave generated in solution by the volumetric changes which follow thermal or structural changes induced by the absorption of light; grating and lensing methods detect changes in the refractive index of a solution due to the thermal, volumetric, or absorbance changes induced by the absorption of light. Recent developments in lensing and grating techniques have dramatically improved the time resolution, providing access to the picosecond time range. On longer timescales, grating and lensing techniques can access effects on the millisecond timescale, and recent instrumental developments with acoustic detection have shown sensitivity in the extended millisecond time range. Curiously, the real time kinetics in the millisecond range, accessed in the first reports on the separation of volume changes of structural origin from those of thermal origin,[1,2] has never been reproduced.

Photothermal methods are usually implemented using laser light sources. The high spectral purity and power, and the spatial beam profile, allow stronger signals to be obtained than with conventional light sources. Coherence is also important in grating-based photothermal methods. Finally, the short time duration of laser light pulses allows time resolution down to the picosecond timescale, which is not achievable with conventional pulsed arc sources.

Several reviews on the principles and the applications of photothermal methods to photochemistry and photobiology have appeared over the last ten years, demonstrating the interest in these methods. The comprehensive review by Braslavky and Heibel[5] still remains a touchstone to refer to for the applications of photothermal methods in photochemistry and photobiology up to 1992. After this review, several others appeared, dealing with applications to supramolecular systems,[8] photosynthesis,[18–20] and various biological molecules.[9,21,22]

This perspective does not aim to be comprehensive, rather it presents the general principles of time-resolved photothermal methods and focuses on some aspects of photochemistry and photobiology that, in recent times, have been fruitfully investigated. The literature we refer to mainly covers the years from 1997 to 2002, but we will often recall previous works in order to illustrate some fundamental points.

2 Photothermal techniques

In the following, we describe the time-resolved photothermal techniques mainly used in photochemistry and photobiology.

2.1 Time-resolved photoacoustic spectroscopy

Laser-induced, time-resolved photoacoustic spectroscopy (PAS), also referred to as laser-induced, time-resolved optoacoustic spectroscopy (LIOAS), monitors the pressure changes induced in a liquid sample after excitation with a (commonly nanosecond) pulsed laser.[5,23] The time evolution of the pressure pulse is monitored by fast piezoelectric transducers, frequently

located in a plane parallel to the direction of the laser beam (right-angle arrangement; Fig. 2).[3–5] Front-face geometry (Fig. 2) is also widely used, especially with strongly absorbing samples. In this arrangement, a dichroic mirror is placed between the cuvette and the transducer to avoid signals generated by direct absorption of the incident light by the transducer's surface.[24–28]

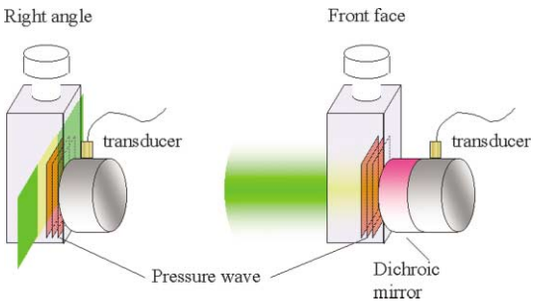

Fig. 2 Comparison of photoacoustic signal generation in the right-angle (left) and front-face (right) geometries. In the right-angle geometry, the pump beam (green) is shaped with a slit to obtain a planar acoustic wavefront.

2.1.1 Description of photoacoustic signal generation. As first proposed by Callis *et al.*,[1] pressure pulses in the illuminated sample arise from the volume changes produced by radiationless relaxation (ΔV_{th}) and structural rearrangements at the molecular level (ΔV_r). Relaxation originates either from non-radiative decay of excited states or heat release (enthalpy change) in photoinitiated reactions, including the heat involved in the rearrangement of the solvent (Fig. 3). The structural volume changes reflect movements of the photoexcited molecules and/or the surrounding solvent in response to such events as dipole moment change, charge transfer, and photoisomerization. Theoretical approaches to understanding photoacoustic signal generation have been developed recently to take into account both experimental arrangements (front-face and right-angle) and the kinetics of non-radiative relaxations.[26,27,29,30]

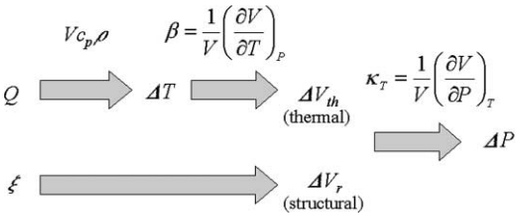

Fig. 3 Enthalpic changes (heat, Q) are converted to changes in temperature through the heat capacity ($VC_P\rho$), and to volume changes of the solution through the isobaric expansion coefficient (β). ξ stands for all molecular, atomic, and electronic rearrangements of solute and solvent molecules leading to a structural volume change. The pressure changes arising from volumetric variations are mediated by the isothermal compressibility (κT).

Using an euristic approach, the overall pressure change can be written as[5,8,31]

$$\Delta P = -\frac{1}{\kappa_T}\left(\frac{\Delta V}{V}\right)_T = -\frac{1}{\kappa_T}\left(\frac{\Delta V_{th} + \Delta V_r}{V}\right)_T \qquad (1)$$

where ΔP is the pressure change, V the illuminated volume, and κ_T the isothermal compressibility. An electrical signal is produced in the transducer, which is proportional to the pressure change.

The signal is also linearly related to the amount of absorbed photons, n_{abs}:

$$n_{abs} = \frac{N_{ph}}{N_A}\left(1 - 10^{-A}\right) \qquad (2)$$

where A is the absorbance of the solution at the excitation wavelength λ, N_A Avogadro's constant, and N_{ph} the number of incident photons. The total signal is given by

$$H^S = kn^S_{abs}\left(\alpha\frac{\beta}{C_P\rho}E_\lambda + \Delta V_e\right) \qquad (3)$$

where $E_\lambda = N_A hc/\lambda$ is the energy of 1 mol of photons of wavelength λ (= 1 Einstein), $\alpha = Q/E_\lambda$ is the fraction of the absorbed energy, E_λ, released as heat, Q, ΔV_e is the structural volume change per absorbed Einstein, C_P the specific heat capacity, ρ the density, and β the cubic thermal expansion coefficient of the solution. For dilute solutions, these properties are those of the solvent. It must be kept in mind that ΔV_e and Q are molar quantities, calculated per mole of absorbed photons. In order to obtain α and ΔV_e, the instrumental constant (k) must be determined by comparing the signal of the sample with that of a calorimetric reference, *i.e.* a system which releases all the absorbed energy as heat in a time shorter than the instrumental response. It is worth recalling that the instrumental constant (k) is inversely proportional to the isothermal compressibility (κ_T). Photocalorimetric reference compounds are substances which are non-fluorescent, show no transients with a lifetime longer than a few nanoseconds, are photochemically stable, and are 100% efficient in delivering the absorbed energy to the medium as heat when the excited molecules return to their ground state. They should not exhibit multiphotonic or ground-state depletion effects at the laser fluence used in the experiment. Several reference compounds have been identified for aqueous solutions and for organic solvents.[5,32] Care must be taken not to use substances with low extinction coefficients at the excitiation wavelength, since for these compounds, high concentrations (mM to M) are needed, which might affect the thermal expansion coefficient. Systematic errors could then be introduced in the data and give erroneous determinations of enthalpic and volumetric changes.[33,34] The calorimetric reference and the sample solutions should be measured under identical experimental conditions, *i.e.* solvent, temperature, excitation wavelength, and geometry. The signal for the calorimetric reference is given by

$$H^R = kn^R_{abs}\frac{\beta}{C_P\rho}E_\lambda \qquad (4)$$

In case permanent products or transient species characterized by lifetimes longer than *ca.* 10 μs are the only products of the photoreaction, the amplitudes of the photoacoustic signals serve to determine the heat and structural volume changes by applying eqn. 5 (obtained from the ratio of eqn. 3 and 4), relating the fluence-normalized LIOAS signal amplitudes for the sample and reference solutions, H^S_n and H^R_n, respectively.

$$\frac{H^S_n}{H^R_n} = \alpha + \frac{\Delta V_e}{E_\lambda}\frac{C_P\rho}{\beta} \qquad (5)$$

For transient species with lifetimes within the pressure integration time, kinetic information is obtained by considering that the signal is a time convolution between the transfer function, $H^R_n(t)$, of the instrument, obtained with the calorimetric reference, and the time derivative, $H(t)$, of the time-dependent ratio H^S_n/H^R_n.[35–37]

$$H^S_n(t) = \int_0^t H^R_n(t')H(t-t')\,dt' \qquad (6)$$

Numerical reconvolution has been used to retrieve the kinetic, enthalpic, and volumetric parameters.[24,36,37] Direct

deconvolution methods have been developed as well.[29] The reconvolution methods assume a sum of single-exponential decay functions for the time evolution of the ratio H_n^S/H_n^R:

$$H(t) = \sum_i \frac{\varphi_i}{\tau_i} e^{-\frac{t}{\tau_i}} \quad (7)$$

where τ_i is the lifetime of transient i and φ_i is its fractional contribution to the measured volume change. This assumption bears no implications regarding the mechanism involved, since several mechanisms lead to a function such as eqn. 7. Lifetimes below a few nanoseconds are integrated in the prompt response, for which it is only possible to obtain the fractional amplitude. Lifetimes between a few nanoseconds and several microseconds can be readily deconvoluted (Fig. 4).

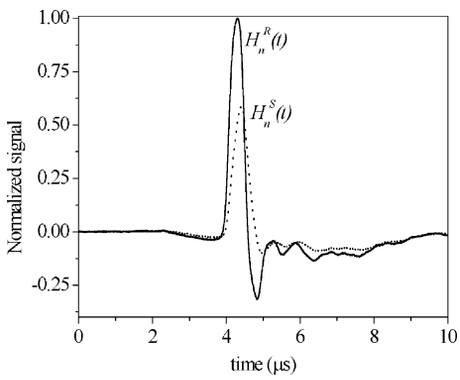

Fig. 4 Photoacoustic signals for aerated acetonitrile solutions of 2-hydroxybenzophenone [$H_n^R(t)$] and benzophenone [$H_n^S(t)$] at room temperature. The signals were measured as described in Murgida *et al.*[38] Both the amplitude and the shape of the signal for benzophenone are different from those for 2-hydroxybenzophenone. The signal for benzophenone, which is thermal in origin, is best described by a double exponential decay with a fast component (lifetime below *ca.* 10 ns), due to triplet formation, and a slower relaxation (lifetime of *ca.* 200 ns), due to triplet quenching by molecular oxygen.

The fractional amplitudes (φ_i) in eqn. 7 contain the heat release (Q_i) and the structural volume change ($\Delta V_{e,i}$) of the ith step. Both contributions can be considered additive provided that the time evolution is the same. This assumption has been validated in several systems.[39] The fractional amplitudes can be written as

$$\varphi_i = \alpha_i + \frac{\Delta V_{e,i}}{E_\lambda}\frac{C_P\,\rho}{\beta} \quad (8)$$

with $\alpha_i = \frac{Q_i}{E_\lambda}$ and $\Delta V_{e,i} = \Phi_i \Delta V_{R,i}$, where Φ_i is the quantum yield of step i. Q_i is related to the enthalpy of the species produced, including the reorganization energy of the medium. $\Phi_i \Delta V_{R,i}$ represents the molar structural volume change of the ith step, which includes intrinsic changes in the chromophore as well as solute–solvent interactions. Eqn. 5 is thus a particular case of eqn. 8 for $i = 1$.

For the proper interpretation of φ_i, a mechanism (parallel, sequential, *etc.*) should be set out in order to relate measured amplitudes to the actual parameters.[36]

2.1.2 Separation of heat release and structural volume change. Separation of the heat dissipation and structural terms in eqn. 8 is achieved by measuring the signals as a function of the ratio $C_P\rho/\beta$.[1,5,31] In aqueous solutions, $C_P\rho/\beta$ strongly depends on temperature (mainly due to the changes in β). Thus, separation of thermal and volumetric contributions is obtained by performing measurements at various temperatures in a relatively small range around room temperature. The ratio $(C_P\rho/\beta)_T$ for neat water is obtained from tabulated values. In particular, $\beta_{H_2O} = 0$ at 3.9 °C ($T_{\beta=0}$), while it is positive above and negative below this temperature. At $T_{\beta=0}$, heat release gives rise to no signal. This peculiar feature allows the straightforward assessment of the existence of structural volume changes. For aqueous solutions containing salts or other additives at mM concentrations or higher, $(C_P\rho/\beta)_T$ and $T_{\beta=0}$ must be determined by comparison of the signal obtained for a calorimetric reference in the solvent of interest and in water.[5]

The precision of the slopes of plots of eqn. 8, $\Delta V_{e,i}/E_\lambda$, is generally good, whereas the intercept, α_i, is affected by larger errors. Where the main goal is the determination of the structural volume change, a two-temperature method may be applied. Essentially, the photoacoustic wave is measured for the sample at $T_{\beta=0}$ and at a slightly higher temperature for which $\beta \neq 0$, $T_{\beta\neq0}$. The parameters $\Delta V_{e,i}/E_\lambda$ and α_i are then calculated with eqn. 9 and 10.

$$\Delta V_{e,i} = \varphi_i(T_{\beta=0})\left(\frac{\beta}{C_P\,\rho}\right)E_\lambda \quad (9)$$

$$\alpha_i = \varphi_i(T_{\beta\neq0}) - \varphi_i(T_{\beta=0}) \quad (10)$$

These equations only hold for values of $T_{\beta=0}$ and $T_{\beta\neq0}$ which are close to each other, such that the risetime of the LIOAS signal and the compressibility of the solution are similar. The signal of the reference at $T_{\beta\neq0}$ is used, together with that of the sample at $T_{\beta=0}$ and $T_{\beta\neq0}$, to obtain the values of $\varphi_i(T_{\beta=0})$ and $\varphi_i(T_{\beta\neq0})$. A time shift of the sample waveform at $T_{\beta=0}$ with respect to the reference waveform at $T_{\beta\neq0}$ is necessary to compensate for the change in the speed of sound that leads to a slightly different arrival time at these temperatures. Thermal instability of the sample holder and trigger arrival fluctuations make the shifting an important option in the fitting routines.

The temperature dependence of $C_P\rho/\beta$ in organic solvents is poor, rendering the above procedures inapplicable to these solvents. This is a major drawback for many photochemical reactions, which cannot be studied in aqueous solvents. The use of aqueous–organic solvent mixtures has been suggested as a possible solution to the separation of enthalpic *vs.* volumetric contributions for compounds which are not water soluble.[40] However, the mixed solvents protocol is also not applicable when the energy of the transient species depends on the solvent polarity, since Q_i (and likely $\Delta V_{R,i}$) changes in the different solvent conditions.

A possible alternative is the use of a series of homologous solvents, such as linear alkanes, in which the term $C_P\rho/\beta$ varies significantly with little change in solvent polarity.[41–43] Cyclic alkanes have been used recently and provide an additional series for the determination of structural volume changes in non-aqueous media.[44] Very recently, a homologous series of aprotic, polar nitrile solvents, consisting of acetonitrile, propionitrile, butyronitrile, and valeronitrile, has been also used.[45] This procedure is valid provided that no significant perturbations are introduced in the photophysics and photochemistry of the solute, and the reaction enthalpy and volume are not changed in the solvent series. These strong assumptions are not necessarily verified. For instance, when charge-transfer reactions occur, according to the continuum dielectric model,[46] both reaction volume and enthalpy would be substantially different across the linear alkane series.[47] This has also been observed for charge-transfer processes in the recently proposed polar nitrile series.[45]

A further method for separating structural from enthalpic volume changes relies on the isotope dependence of $C_P\rho/\beta$. For instance, $C_P\rho/\beta$ is increased by a factor of 2 for D_2O compared to H_2O.[5] The relative variation of this parameter between D_2O and H_2O is larger than is observed in the series of linear alkanes. It is expected that this subtle variation in solvent

composition will not result in appreciable effects, apart from cases where proton-transfer reactions occur.[47]

2.1.3 Calorimetric calculations. The heat released in each step (Q_i) is interpreted in terms of enthalpy changes by using the energy balance (eqn. 11),[5,23] where the input energy (E_λ) is equal to the sum of the energy released as emission (*e.g.* fluorescence; Φ_i and E_λ are the quantum yield and energy of the emitting state; phosphorescence is neglected) and the heat dissipated (changes in the states energy content plus energy associated with solute–solvent interactions) in each of the steps. E_{stored} represents the energy trapped in species living much longer than the pressure-integration time of the experiment.

$$E_\lambda = \Phi_f E_f + \sum_i Q_i + E_{\text{stored}} \qquad (11)$$

Analysis of the calorimetric information requires knowledge of the reaction scheme and the parameters associated with the process, such as quantum yields and energy levels derived, for example, from optical measurements.

2.1.4 Instrumental developments. A few instrumental developments have been proposed recently, mainly aimed at reducing the sample volume and increasing the sensitivity. As already mentioned, two different experimental geometries are commonly used in pulsed PAS, the traditional cuvette cell with the piezoelectric detector acoustically coupled parallel to the incident excitation beam, and the more recently developed front-face irradiation, with the piezoelectric detector acoustically coupled to a dielectric reflector normal to the incident excitation beam. The cuvette geometry is still the preferred experimental choice for the analysis of weakly absorbing solutions due to the inherent zero background. Recently, use of a rectangular excitation beam profile has resulted in improved sensitivity with respect to the more common circular shape, for which the amplitude of the resulting acoustic wave decreases inversely with distance between the excitation source and detector. Front-face irradiation still provides better sensitivity and time resolution[48] for strongly absorbing solutions.

Pulsed PAS is a technique of greatest interest for detection trace levels of compounds,[49–51] its sensitivity being a factor of 100–1000 higher than conventional absorbance spectroscopy.[3] Sensors based on photothermal techniques have been designed to monitor Cr(VI) in water,[51] pH and CO_2,[52] and water in oil.[50] Tunable microsecond flashlamps have been recently introduced in the PAS set-up in order to obtain excitation wavelengths over a broad spectrum.[53] This, together with the use of low frequency transducers and standard data acquisition boards, has resulted in substantiallly reduced detection costs. Under these conditions (long excitation pulse), the detection limit is dictated by solvent absorption.

Despite the claims that PAS can also be used for studies with strongly scattering samples, quantitative analysis of the photoacoustic waveforms is particularly critical when light scattering is very intense. However, a peculiar feature of PAS experiments in the presence of light scattering has been recently turned into a potential resource. Scattering samples (as well as strongly fluorescent samples) are known to generate a 'spurious' acoustic wave due to the absorption of scattered light by the transducer's surface. This signal, along with the 'normal' acoustic wave coming from absorbance in the solution, has been used to quantitate absorbance and scattering from a colloidal silica solution.[54] Comparison with spectrophotometric data has shown that the determination of absorbance using this method is potentially superior.

Several new experimental arrangements for reduced sample volumes have been proposed. Autrey *et al*. have described a nanoliter time-resolved calorimetric experimental approach using a photoacoustic cell made from narrow bore, flexible, fused silica capillary tubing.[55] The fused silica capillary permits the transmission of an excitation source from the far UV to the near infrared. This geometry has proven to be capable of detecting with high sensitivity kinetics in the nanosecond range and allowed pressure-dependent investigations (*vide infra*). Similar approaches based on capillary tubing have been proposed for photothermal beam deflection set-ups.[56]

An extremely promising cell for pulsed PAS that uses transmission of light through a pair of dovetail prisms has also been described.[57] The layered prism cell combines the enhanced time-resolution capabilities of the 'layered' front-face irradiation geometry with the zero background and broadband flexibility of the classical cuvette geometry. This detection method has proven to have increased sensitivity and time resolution as compared to both right-angle and front-face detection. Among other advantages of the method, it is worthwhile noting that the acoustic transit time is negligible and the arrival time to the transducer of the acoustic waveform is independent of the thermoelastic properties of the solution and, consequently, of temperature. However, despite its great promise, there has been no new application of this method to photobiological and photochemical problems since its first description.

A high pressure photoacoustic calorimeter has been recently developed to operate up to 200 MPa and investigate microsecond kinetics and thermodynamics of reactions in solution.[58,59] Both thermal expansion and the volume of reaction contribute to the generation of the photoacoustic signal, and the separation of these contributions has been achieved by variation of the pressure. The method has been demonstrated for the determination of the enthalpy and volume of reaction for diphenylcyclopropenone decomposition to diphenylethyne and carbon monoxide.[58] The photoacoustic signal for chromium hexacarbonyl and acetonitrile in heptane was also examined from near ambient pressure to 100 MPa and the enthalpy and the volumes of heptane displacement from chromium pentacarbonyl heptane were determined.[59] Other high pressure studies carried out using a photoacoustic technique include the characterization of the enthalpy changes of the reactions $M(CO)_6 \longrightarrow M(CO)_5(L)$ (M = Cr and Mo; L = H_2, and N_2) in *n*-heptane and the photosubstitution of $(\eta_6\text{-}C_6H_6)Cr(CO)_3$ by *n*-heptane, H_2, and N_2, which have been studied with a high pressure photoacoustic set-up (130 bar of H_2 or N_2) to increase the concentration of H_2 or N_2 dissolved in the solvent, thereby accelerating the reactions.[60,61]

Acoustic detection of millisecond transients was achieved more then 20 years ago by Parson and co-workers[1,2] but after their pioneering work, the technique was never applied again. Recently, proposals have been made to access longer timescales by using broadband detectors.[62,63] However, data retrieval is still far from being straightforward.

2.2 Photorefractive techniques

When a sample is excited with a light beam being absorbed by the sample—the so-called pump beam, which usually has a spatially Gaussian shape—the concentration of the excited-state molecules reflects the pump beam geometry. The non-radiative relaxations of the excited states heat the sample, resulting in a temperature profile which reflects the Gaussian intensity profile of the exciting laser beam. The increased temperature decreases the density and, as a consequence, the refractive index of the sample as well. As discussed later on, other sources of photoinduced refractive index changes also play an important role. Three basic experimental approaches to detecting the refractive index change exist: (i) transient lens (TL), (ii) beam deflection (BD), and (iii) transient grating (TG). TL, TG, and BD are also known by different names for historical reasons, since, originally, the heat release—and subsequent temperature increase—was erroneously thought to be the only/major signal contribution. Therefore TL and TG stand also for

thermal lensing and grating, respectively, while BD is usually referred to as photothermal BD (PBD).

A light beam of lower intensity and different wavelength to the pump beam—the probe beam—travelling through the illuminated region is expanded by the Gaussian profile of the refractive index and this effect can be detected from the change in light intensity through a pinhole placed in the far field (Fig. 5). This detection scheme is used in the TL method.

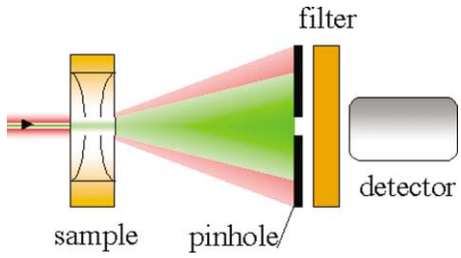

Fig. 5 Principles of collinear TL signal generation. In transient lensing, the pump (green) and probe (red) beams are collinear and concentric. The transient lens induced in the sample as a result of the refractive index change following pump beam absorption defocuses the probe beam. This defocusing is detected as a reduction in the amount of probe beam power striking the photodetector.

If the probe beam is not perfectly concentric with the pump beam, the spatial profile of the refractive index results in deflection of the probe beam, rather than expansion. In this case, a position-sensitive detector (usually a dual-element photodiode) monitors the displacement of the probe beam. This is the BD detection scheme (Fig. 6). A major difference between TL and BD is that while TL requires a nearly ideal Gaussian beam profile for the pump laser, this requirement is not so stringent for PBD.

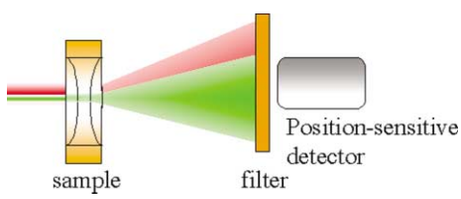

Fig. 6 Principles of BD signal generation. In the collinear photothermal beam deflection, the pump (green) and probe (red) beams are collinear and offset. As a result, the transient lens that develops deflects the probe beam through an angle. This deflection is detected as a change in the position of the probe beam spot on the position-sensitive photodetector.

In TG, two laser beams with parallel polarization are brought into the sample at a certain angle (θ) and, depending on their interference pattern, a modulation of the excitation intensity results. The refractive index changes originating from the photoinduced processes reflect this modulation, and can be monitored by a third laser beam, which is diffracted to an extent which depends on the grating properties (Fig. 7).

The above qualitative description of the signal generation, however, does not take into account several possible sources of refractive index changes of non-thermal origin, which, in many cases, may be a substantial part of the measured effect. These effects, discussed below, include the optical Kerr effect, changes in concentrations of solutes, absorbance, and partial molal volume due to the induced photochemistry, and electrostriction.[64]

In their traditional application, the time resolution of TL and PBD is determined by the mechanism of generation of the lens. To form the lens after a fast non-radiative relaxation, it takes a characteristic time for the medium to expand in response to the heat released. This time is given by $\tau_{ac} = w/v$, where w is the beam radius and v the speed of sound in the medium. With a reliable experimental set-up, this time is approximately 100 ns, which sets the lower limit for the access-

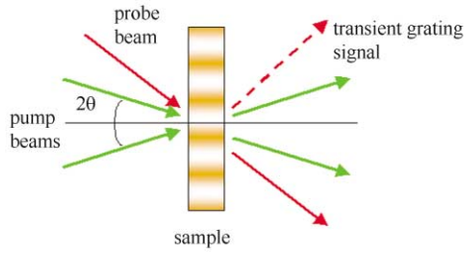

Fig. 7 Principles of TG signal generation. A sinusoidal modulation of the excitation light intensity (green arrows) inside the sample is produced by the interference of two light waves with parallel polarization. The non-radiative processes following absorption of light create the sinusoidal modulation in the refractive index (n) and the absorbance (k). The grating is monitored by the diffraction efficiency of another time-delayed laser pulse or continuous wave (cw) laser (red arrows).

ible timescales.[6,64,65] On longer timescales, a millisecond limit exists due to the thermal diffusion across the illuminated area.

TG can provide a time resolution of about 30 ps.[65–69] This inherent response originates from the fact that TG, as with most of the photothermal detection methods, uses the matrix density change caused by the temperature increase as the source of the signal. Therefore, the time resolution is determined by the acoustic propagation time over the fringe spacing (Λ, usually in the hundreds of nanometers to the tens of micrometers range) of the grating, $\tau_{ac} = \Lambda/v$, where v is the sound velocity. While investigating the kinetics of energy flow from solute to solvent, Terazima and co-workers recently introduced a further improvement in time resolution by proposing several new refinements in the detection set-up.[64,65,70–75] Depending on experimental conditions, the resolution can reach a few picoseconds.[65]

2.2.1 Description of TL and BD signal generation. The transient lens signal can be understood as arising from the formation of a refractive index lens.[64] Due to the interaction between the electromagnetic field of the incident (pump) beam and the sample, the complex refractive index varies through the third order of optical nonlinearity as

$$\delta n(r,t) = \int_{-\infty}^{t} \frac{\mathrm{d}t' 6\chi^{(3)}(t') E_{\mathrm{pump}}^{2}(r)}{2n_0} \qquad (12)$$

where $\delta n(r,t)$ represents the overall variation of the refractive index and n_0 is the relaxed refractive index. For a Gaussian-shaped pump beam, a time-dependent Gaussian profile of the refractive index results:

$$\delta n(r,t) = n(r,t) - n_0 = -\delta n(t) \exp\left(\frac{-r^2}{w^2}\right) \qquad (13)$$

where w is the excitation beam radius and r the distance from the center of the pump beam.

The signal at the detector will be proportional to the refractive index change and can be calculated according to the theoretical treatments already developed.[6] For instance, for the detection configuration reported in Fig. 8, the time-dependent lens signal can be calculated as[64]

$$S(t) = \frac{I[n(t)] - I[n(t<0)]}{I[n(t<0)]} = \frac{4fL\delta n(t)}{w^2 n_0} \qquad (14)$$

where $I[n(t)]$ and $I[n(t < 0)]$ are the intensity of the probe beam through the aperture at a given delay time, t, and slightly before the pump laser pulse, respectively, f is the focal length of the external lens used to expand the probe beam, and L the

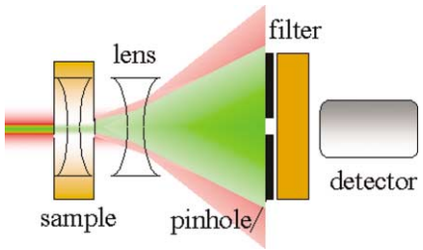

Fig. 8 One possible TL signal detection configuration.[64] A concave lens is placed between sample and detector so that the probe beam is expanded. After travelling a certain distance, the center of the beam is passed through a pinhole and its intensity detected.

thickness of the sample. If d' is the distance between the sample and the external lens, and d is the distance between the lens and the pinhole, it is assumed that $L + d' \ll f \ll d$.

The above description applies to refractive index changes due to all possible sources. However, due to the different nature of the effects contributing to changes in refractive index, the timescale of the appearance of the signal can be substantially different.

As already observed, the TL and BD techniques are closely related. It is expected that the sources giving rise to the lens signal also contribute to a beam deflection signal. However, BD is a much less well explored detection technique than TL and, therefore, the potential of the technique has not yet been completely established. A major advantage of BD over TL is that beam deflection generation does not require a Gaussian pump beam and, therefore, allows gas lasers as excimers and nitrogen lasers to be used.[7,76] Collinear co- or counter-propagating pump and probe beams have been employed, the latter geometry showing some advantages when working with intense UV laser pump sources.[7] The sensitivity of collinear BD (as well as TL) has been proven to be higher than for transverse excitation, although the latter arrangement is easier to align.[6,7] Recent experiments using right-angle geometry have achieved better sensitivity by shaping the pump beam with a knife-edge, which produces an angle to the probe beam.[77,78]

Transient lens, beam deflection, and transient grating (*vide infra*) signals have a time range of applicability which may be different depending on the source of the signal being considered (*vide infra*), spanning from a few picoseconds to several milliseconds. Due to the low rate of formation of the density lens (~10^7 s^{-1}), TL and BD do not have the capability to access the 10^{-7} s range typical of pulsed PAS detection and, in this sense, they are complementary to the acoustic method. On the other hand, these techniques are very sensitive in detecting slower kinetics, extending to the millisecond timescale, as well as detecting much faster variations in refractive index not related to density changes. Finally, these techniques share a common advantage with respect to acoustic detection; the capability of reproducing real time kinetics free from a complex detection response, such as is observed for piezoelectric transducers. Recent theoretical work has shown that, in the case of grating techniques, detection of second-order reaction kinetics may not be trivial, although careful analysis showed that quantitative thermodynamic information can also be retrieved in this case.[79]

In order to retrieve quantitative thermodynamic informations from the lens and beam deflection signals, a photocalorimetric reference must be used to calibrate the instrumental response, in essentially the same manner already described for the photoacoustic signals. The signal, $R(t)$, for a photocalorimetric reference compound (releasing all of the absorbed energy as heat) is measured under the same experimental conditions (temperature, laser pulse energy, absorbance, solvent) used for the sample under investigation. The reference compound should show no refractive index changes due to sources other than heat release. The requirement for the reference compound to release the absorbed energy as heat within timescales which are short compared to the risetime of the detection method under use is not stringent. It is nevertheless useful to have fast heat release, since it helps to set the actual time resolution of the technique.

The signal of the reference compound, as well as the signal of the sample, $S(t)$, are usually normalized for laser pulse energy (E) and for differences in the absorbance of the samples ($1–10^{-A}$).

The amplitude of the sample signal can be calibrated from the ratio of the signals normalized for absorbance and laser pulse energy:

$$s(t) = \frac{S_n(t)}{R_n(t)} \tag{15}$$

Due to the characteristics of the signal, for which no deconvolution is needed, it is expected that more complex kinetics can be retrieved than with time-resolved PAS.

2.2.2 Description of TG signal generation. The transient grating signal can be described as arising from an intensity grating of the pump beam. A sinusoidal modulation of the light intensity is produced by the interference of two light waves with parallel polarization. The fringe spacing (Λ) is given by

$$\Lambda = \frac{\lambda_{ex}}{2\sin\theta} \tag{16}$$

where θ is the angle between the two excitation beams and λ_{ex} the wavelength of the excitation laser. The interaction of light with the sample creates the sinusoidal modulation in the refractive index and absorbance through several effects, in exactly the same way described for transient lens generation. The time evolution of the grating is monitored by the diffraction efficiency of another time-delayed laser pulse for probe times shorter than about 10 ns, or a cw laser beam for longer timescales. For a thick grating, the probe is brought in at an appropriate angle to satisfy the phase-matching condition (the Bragg condition). Under a weak diffraction condition, the diffraction intensity (I_{dif}) is proportional to the square of the variations in the refractive index and absorption:[80]

$$\frac{I_{dif}}{I_0} \approx \exp\left(-\frac{A\ln 10}{\cos\theta}\right)\left|\frac{\Delta\tilde{n}\pi d}{\lambda_{pr}\cos\theta}\right|^2 = C\left|\Delta\tilde{n}\right|^2 \tag{17}$$

where I_0 is the probe laser intensity, A the absorbance at the probe wavelength (λ_{pr}), d the sample thickness, and $\Delta\tilde{n}$ the modulation amplitude of the complex refractive index. C is a proportionality factor encompassing all the constants. The weak diffraction condition implies $I_{dif}/I_0 < 10^{-2}$.

The sources of the grating are ultimately the sources of the refractive index changes and, therefore, the description outlined for lensing can be applied to the grating method.[64,65]

$\Delta\tilde{n}$ is a complex quantity which can be split into the modulation amplitude of the real refractive index (Δn) and of the attenuation index (ΔK):

$$\Delta\tilde{n} = \Delta n + i\Delta K \tag{18}$$

and the absorbance is related to ΔK by $\Delta K = 1.15\lambda\Delta A/2\pi d$. Using this expression, the diffracted intensity can be written as

$$\frac{I_{dif}}{I_0} \approx C\left|\Delta n^2 + i\Delta K^2\right| \tag{19}$$

The contribution of Δn to the total diffracted intensity (I_{dif}) can be estimated only if the phase of the signal is known.

This information is generally retrieved by performing optical heterodyne detection.[80,81]

2.2.3 Separation of various contributions to the refractive index change. Several effects contribute, on different timescales, to the observed changes in refractive index being monitored in the TL, BD, and TG methods. This renders the identification of the various contributions more complex than early investigations assumed. Nevertheless, this drawback can be turned into a peculiar advantage to access phenomena otherwise hardly detectable.

Overall, the change in refractive index can be written explicitly as a sum of the different contributions normally observed:[8,64,65,82,83]

$$\delta n = \left(\frac{\partial n}{\partial \rho}\right)_T \left(\frac{\partial \rho}{\partial T}\right) \delta T + \left(\frac{\partial n}{\partial T}\right)_\rho \delta T + \left(\frac{\partial n}{\partial V}\right)_T \delta V + \delta n_\kappa + \delta n_{\mathrm{OK}} \quad (20)$$

The first two terms are due to the heat release upon radiationless decay of the photoinduced transient species and express the density and the temperature lens terms, respectively. The third term contains the density lens due to the structural volume changes. δn_k represents the change in refractive index on changing the absorbance and δn_{OK} the refractive index change due to the optical Kerr effect.

Density lens. The density-mediated refractive index changes due to heat transfer to the medium are formed with a time constant dictated by the acoustic transit time ($\tau_{\mathrm{ac}} = w/v$) of the experimental arrangement. The density change can be separated into an acoustic mode, responsible for the first appearance of a signal pulse (Fig. 9), and a diffusive mode (Fig. 10), dominating the slower part of the lens signal. This signal decays with a time constant characteristic for the diffusion of the heat outside the illuminated area. In cases where the heat transfer is much slower than the time development of the acoustic pulse, its kinetics can be extracted from the diffusive part of the signal. If the kinetics is faster than or comparable to the acoustic transit time, the acoustic peak masks the heat-releasing process and the kinetics cannot be determined from the rise part of the signal. It has been repeatedly found that the time resolution of the signal is then around 100 ns. This contribution is the 'normal' thermal source of the signal used in photocalorimetric applications employing nanosecond lasers. The decay of the signal due to heat diffusion occurs within about 100 ms, depending on the pump and probe beam diameters. Transients with lifetimes below τ_{ac} are not resolvable by these methods and, for these applications, pulsed PAS is the technique of choice.

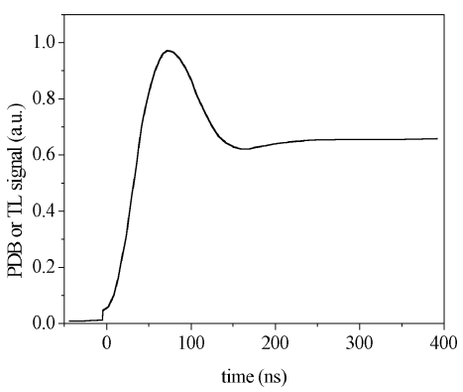

Fig. 9 A typical temporal profile of the rising part of the density lens signal, showing the acoustic peak with risetime of the order of 100 ns. The first tiny step increase is due to the temperature lens (*vide infra*).[64,65]

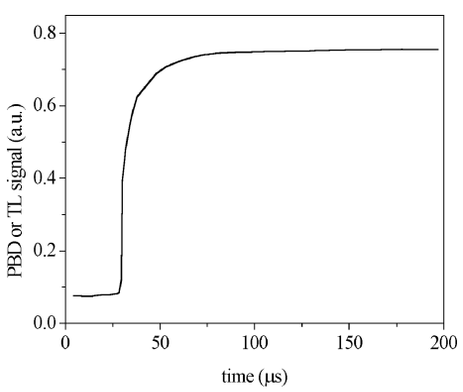

Fig. 10 A typical temporal profile of the diffusive part of the density lens (or beam deflection) signal, showing a fast, unresolvable rise of the signal and a slower kinetics in the tens of microseconds region.[76]

Population lens. The population lens has been introduced to describe the refractive index changes due to the change in polarizability between the ground and excited states, leading to changes in the absorbance of the sample after photoexcitation.[8,82,83] The dispersion range of the refractive index is much wider than the absorption spectrum range and it is common to observe this contribution at probe wavelengths far from the absorbance range. Even though this effect renders the signal more complex, it turned out to be an interesting tool for the investigation of excited-state dynamics. The absorption spectrum and the refractive index change are connected by the Kramers–Kronig relation:

$$\delta n = \frac{N_1}{2n_0} \sum_i \frac{4\pi e^2 f_i \left(\omega_i^2 - \omega^2\right)}{m\left[\left(\omega_i^2 - \omega^2\right)^2 + \gamma_i^2 \omega^2\right]} \quad (21)$$

where m and e are the mass and charge of an electron, respectively, f_i is the oscillator strength of the ith band, ω_i and γ_i are the frequency at the absorption maximum and the bandwidth of the ith band, respectively, and N_1 is the number density of the excited state. This signal is observed whenever excited states or reaction intermediates persist on the timescale of the thermal lens experiment.

The photoinduced changes in the absorption of the sample produce changes in the refractive index in all spectral regions, even those far from the ground state and transient species absorbances. In order to avoid interference to the refractive index changes due to the changes in absorbance, the probe beam wavelength has to be red-shifted as far as possible with respect to the edges of any absorbances due to reactants, intermediates, and products. In experiments with sub-nanosecond pulses, some information on the contributions from absorbance changes can be obtained by using polychromatic probe light pulses.[80,84]

Optical Kerr lens. The strong electromagnetic field of the laser pulse distorts the electronic distribution of the molecule by aligning the most polarizable axis, thus anisotropically changing the refractive index. This effect, observed essentially on the femtosecond to picosecond timescale, can be separated into a fast electronic and a slower nuclear term by means of polarization-dependent experiments.[85,86]

Temperature lens. The change in refractive index as a function of the variables T and ρ can be written as

$$\delta n = \left[\left(\frac{\partial n}{\partial \rho}\right)_T \left(\frac{\partial \rho}{\partial T}\right) + \left(\frac{\partial n}{\partial T}\right)_\rho\right] \delta T \quad (22)$$

where the first term is the refractive index change accompanying the change in density due to the thermal expansion of the medium (density lens) and the second term is a change not implying a density variation. The most notable difference between the first and second terms is the response time of the signal. While the density lens is formed with a time constant of around 100 ns, the temperature lens has a risetime comparable

with that of the temperature increase. Although the magnitude of the second term is small compared with the first term, clear evidence of its contribution on short timescales in water has been obtained.[70,71,87] In organic solvents, the first term is a factor of 10 larger than the second and it is difficult to evidence it in the resulting signal.

The acoustic signal due to the density lens dominates the TL and BD signals, and it disturbs any fast detection of the temperature rise. However, when this contribution can be made negligibly small, the second term affords a time resolution no longer limited by the medium expansion time but only by the duration of the excitation pulse. Although the temperature lens signal should have acoustic and diffusive parts, as with the density lens, the acoustic part is very small and does not substantially influence the risetime of the temperature lens (Fig. 11).[88]

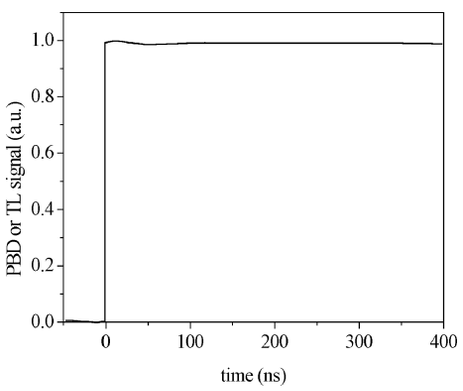

Fig. 11 A typical temporal profile of the rising part of the temperature lens signal, showing the much faster response compared to the density lens signal. A very small acoustic mode is present also in this term, which shows up as the tiny modulation of the signal below 100 ns in this figure.[64,65]

In aqueous solutions, the temperature lens can be evidenced by making the contribution of the first term null through the term $\partial\rho/\partial T$. At $T = 4$ °C, the density is at a maximum and the temperature derivative vanishes, leaving the term $(\partial n/\partial T)_\rho$ as the only thermal source of signals.[64,88] On timescales longer than the risetime, the two terms can be treated as one:

$$\delta n = \frac{\mathrm{d}n}{\mathrm{d}T}\delta T \tag{23}$$

Volume lens. If photoexcitation leads to changes in the molar volumes of the solutes, density changes and an alteration of the refractive index results. The volume lens is formed in essentially the same way as the density lens of thermal origin is formed, *i.e.* through the compressibility of the medium.

Time evolution of TL and probe BD signals. For times greater than τ_{ac}, two regimes can be identified. For beam diameters of 100 μm and in aqueous solutions, heat diffusion can be neglected and the signal can be written as[5]

$$S(t) = C_1 E_a \Phi\left[\left(\frac{\partial n}{\partial \rho}\right)_T \left(\frac{\partial \rho}{\partial T}\right)\frac{1}{\rho C_P} Q(t) + \rho\left(\frac{\partial n}{\partial \rho}\right)_T \Delta V_e(t) + C\Delta n_\kappa(t)\right] \tag{24}$$

C_1 is an instrumental constant and is determined using a photocalorimetric reference of matched absorbance, E_a the absorbed energy, Φ the quantum yield, Q the heat release, ΔV_e the structural volume change, C is a proportionality constant, and Δn_κ the refractive index change due to transient absorbance.

For a photocalorimetric reference compound, we have $Q = N_A h\nu$, therefore,

$$R(t) = C_1 E_a\left[\left(\frac{\partial n}{\partial \rho}\right)_T \left(\frac{\partial \rho}{\partial T}\right)\frac{h\nu}{\rho C_P}\right] \tag{25}$$

On longer timescales (ms), the influence of heat conduction can be corrected for by using the signal of a photocalorimetric reference.[5,8,83]

Protocols for separating the sources of refractive index change. From eqn. 20 it appears clear that achieving separation of the various contributions to the TL, BD, and TG signals is more complex than for PAS.

Zimmt and Vath proposed a method for separating thermal signals from non-thermal signals for reactions with a thermal contribution which decays faster than the risetime of the density lens.[47] As already described, for the density changes, eqn. 22 holds. In organic solvents, the first term tends to generate much larger changes in the refractive index than the second term. However, the term $(\partial n/\partial T)_\rho \delta T$, which gives the time profile of the temperature increase, exactly tracks the heat released because equilibration amongst the vibrational, rotational, and translational modes of the solvent is usually extremely fast.[89] The first term, $(\partial n/\partial \rho)_T(\partial \rho/\partial T)\delta T$, which represents the density contribution to the signal, has a much slower response. Refractive index changes due to changes in the molecular volume are mediated by density changes and have the same limitations in time response as the thermal contribution, $(\partial n/\partial \rho)_T(\partial \rho/\partial T)\delta T$. If a reactive species is formed and decays before the density-mediated refractive index changes occur, then the ratio of the heat released in the formation and decay processes can be determined. Absolute reaction enthalpies can be determined through variation of the excitation wavelength.[47] However, it has been suggested that the method will have very stringent requirements for the experiment to be feasible in organic solvents. It has been estimated that in solvents such as ethanol and cyclohexane, the term $(\partial n/\partial T)_\rho \delta T$ will account for less than 1% of the whole signal, thus requiring a tenfold increase in excitation pulse energies and the absolute absence of signals deriving from transient absorption (δn_k).

Another protocol for the separation of the different refractive index sources takes advantage of the strong temperature dependence of the first term in eqn. 20 in aqueous solutions. This term can be made negligible in aqueous solutions by acquiring the signals at the temperature for which $(\partial n/\partial \rho)_T(\partial \rho/\partial T)\delta T = 0$. Experiments performed at several temperatures allow the parameter to be varied over a relatively large range and enthalpy changes can be separated from structural volume changes and transient absorbance.[5]

Some strategies have been proposed for the separation of structural volume changes from the term arising from transient absorbance. For chromophoric systems with rotational diffusion times longer than that required for the completion of the photoinduced process, it is possible to evaluate the term containing Δn_κ by combining lensing (or BD, or TG) and transient absorbance experiments with linearly polarized pump and probe light beams.[83]

Terazima and co-workers proposed a hybrid method using transient grating and photoacoustic detection to obtain the enthalpy and the structural volume change separately.[90–94] The contributions of ΔV and ΔH can be separated in a time-resolved manner without any temperature and solvent variations.

If the absorptive contribution is negligible, the TG signal intensity is proportional to the square of the peak-null difference of the refractive index in the grating pattern. There are two main contributions to the refractive index change: the thermal effect and a change of chemical species by the reaction

$$I^{1/2}(t) = Z\left|\delta n_{th}\exp\left(-q^2 D_{th} t\right) + \sum_i \delta n^i_{spe}\exp\left(-q^2 D_i t\right)\right| \tag{26}$$

where q is the grating wavenumber, D_{th} the thermal diffusivity, D_i the diffusion coefficient of species i, and Z a proportionality constant. δn_{th} and δn^{i}_{spe} are the magnitudes of the refractive index changes caused by the heat released from the excited state and formation (or extinction) of species i, respectively.

There are two contributions to δn^{i}_{spe}, namely the refractive index changes due to the changes in the absorption spectrum (population grating) and the molecular volume (volume grating). Since D_{th} is usually one or two orders of magnitude larger than D_i in solution, the thermal component can be separated from the grating of non-thermal origin. The magnitude of the thermal grating is given by

$$\delta n_{th} = \frac{dn}{dT}\frac{N_A h\nu \phi W}{\rho C_P}\Delta N \qquad (27)$$

where $\phi = 1 - \frac{\Phi \Delta H}{N_A h\nu}$, W is the molecular weight, C_P the specific heat capacity, ρ the density, $h\nu$ the photon energy of the excitation light, ΔN the number of reacting molecules in the unit volume, and Φ the reaction quantum yield. ΔH can be determined by comparison with the signal intensity of a reference sample. Taking the ratio of the refractive index change for the sample to that for the reference gives

$$\frac{\delta n_{th}^{sample}}{\delta n_{th}^{reference}} = 1 - \frac{\Phi \Delta H}{N_A h\nu} \qquad (28)$$

With the value of $\Phi\Delta H$ from the thermal grating, it is possible to retrieve the structural volume change, $\Phi\Delta V$, from the PAS data at the same temperature at which the thermal grating signal was measured. It is clear from the above that this method applies only to fast, sub-resolution transients. The method has been applied to study the photodissociation of diphenylcyclopropenone[90,91] and diazo compounds.[92]

Finally, it has been suggested that fast structural changes may generate a grating signal with a rate constant different from the rate at which the density grating of thermal origin is formed.[95] However, unequivocal experimental confirmation of this is still missing.

If the retrieval of thermodynamic information from PAS, TL, and BD is fairly well established (apart from possible problems in separating the different sources of the signals), this is not the case for grating techniques.[96] Signal amplitudes in PAS and lensing techniques are converted to enthalpy and volume changes by refering to calibrating compounds (photocalorimetric references). Although, in principle, the same procedure could be applied to retrieve enthalpic information from grating signals, the complexity of the method (several optical beams, sensitivity to beam replacement and intensity, and long acquisition times) makes quantitative comparisons of absolute signal amplitudes from independent transient grating experiments difficult. To overcome this problem, an internal calibration/mixtures method was reported for the determination of short-lived intermediates.[96] Excitation and analysis of thermal phase grating waveforms from mixtures containing both a calibration compound and a precursor to a reactive intermediate of interest provides a value for the total heat release for the formation and decay of the reactive intermediate in the time window of the experiment. Absolute reaction enthalpies for formation and decay of the intermediate of interest can then be calculated.

3 Applications

3.1 Electron transfer: testing electrostriction and specific molecular interactions

Electron-transfer reactions in solution are accompanied by internal molecular changes as well as by solvent rearrangements. Internal changes are the result of variations in bond lengths and angles, whereas solvent reorganization may be due to changes in the distribution of charges (electrostriction effect) and/or to changes in specific solute–solvent interactions concomitant with the electron-transfer reaction. It is, therefore, not surprising that photothermal methods have provided valuable information about the energetics and dynamics of these processes. In addition, results obtained using photothermal methods have provided a testbed for the applicability of simple continuum electrostatic models to the description of the electrostrictive forces acting on solvated ions.

Arata and Parson found a strong contraction (*ca.* −20 mL mol^{-1}) of the solution accompanying charge separation in the electron-transfer reaction from P-870 to quinones in *Rhodopseumonas sphaeroides* reaction centers, which they suggested could arise from electrostriction of the separated charges.[2] At the time, however, the mechanistic origin of the observed contraction was just theoretical. It is only recently that these processes have been more thoroughly investigated using pulsed PAS in a series of works by the groups of Braslavsky[11,12,97–100] and Mauzerall.[28,101–109] Time-resolved PAS was used to investigate, amongst other things, the quenching of porphyrin triplets by quinones,[103] the quenching of the triplet metal-to-ligand charge-transfer (^{3}MLCT) state of Ru(bpy)$_3^{2+}$ by various Fe(III) salts,[100] the electron-transfer reaction between the metal-to-ligand charge-transfer triplet state of Ru(bpy)$_3^{2+}$ and the methyl viologen cation (MV^{2+}),[12] and the reaction of triplet-state zinc uroporphyrin (ZnU) with ferricyanide ions.[108] Electron transfer in photosynthetic systems is reviewed below.

The data accumulated so far evidence that simple continuum electrostrictive models sometimes cannot account for the observed contractions, especially when dealing with small ions[110] and systems undergoing specific, charge-dependent solute–solvent interactions.

The classical continuum approach describing the contraction (ΔV_{el}) of a solution was given by Drude and Nernst:[46]

$$\Delta V_{el} = \frac{(ze)^2}{2r\varepsilon}\frac{\partial \ln \varepsilon}{\partial P} \qquad (29)$$

where ze is the charge of the ion, ε the dielectric constant of the medium, r the radius of the ion, and P the pressure. However, application of this equation often fails to describe the observed volume changes. The reasons for this failure have been found in specific solute–solvent interactions[11,12,100] or in the difficulty of defining the correct parameters for use in eqn. 29.[108] For instance, the volume change observed for the electron-transfer reaction of triplet-state ZnU with ferricyanide ions could not be completely described by the Drude–Nernst equation, which predicts a volume change of about half the observed value. The failure was partially accounted for by employing a saturation function for the orientation polarization of the water dipoles in the electric field of the ions using the integral form of the Drude–Nernst equation.[108]

The quenching of the triplet state of zinc tetraphenylporphine by oxygen and 1,4-benzoquinone was studied using laser-induced optoacoustic spectroscopy in a homologous series of polar, aprotic nitrile solvents, consisting of acetonitrile, propionitrile, butyronitrile, and valeronitrile.[45] The inverse correlation between the oxygen quenching efficiency of triplet-state zinc tetraphenylporphine and the efficiency of singlet oxygen formation, against solvent polarity, was attributed to formation of a charge-transfer complex during the quenching process. No structural volume change was observed for the formation of triplet-state zinc tetraphenylporphine using the nitrile variation method, whereas electron transfer between zinc tetraphenylporphine and 1,4-benzoquinone resulted in a solvent-dependent volume contraction. The observed contractions were explained with specific solute–solvent interactions

and electrostriction. The reason for the solvent-dependent solute–solvent interaction was found to be the variable strength of the interaction between the electron pair donor nitriles and the zinc tetraphenylporphine cation across the solvent series. The free energy of the electron transfer was, however, very similar within the solvent series.

Intramolecular electron-transfer reactions have been also investigated for flexible[111] and rigid[112] donor–acceptor compound in a series of alkanes. The charge-transfer states formed in the molecules are characterized by giant dipole moments, leading to observed ΔV_{str} values of the order of -100 mL mol^{-1} for the rigid molecule, which were dependent on alkane length and temperature. These remarkably large contractions were interpreted as arising from electrostrictive forces on the alkane solvent around the dipolar charge-transfer species and were in agreement with what was predicted by classical electrostatic theory for dipolar molecules:

$$\Delta V_{el} = -\frac{\mu^2}{r^3}\frac{(\varepsilon+2)(\varepsilon-1)}{(2\varepsilon+1)^2}\kappa_T \qquad (30)$$

where μ is the dipole moment of the molecule, r the radius of the molecule, and κ_T the compressibility of the medium. In the case of the flexible compounds there is an additional contribution (apart from the solvent reorganization) to the observed contraction, that might be attributable to the conformational change taking place upon exciplex formation.

For the intramolecular electron transfer associated with formation and decay of the ^{3}MLCT state of Ru(bpy)CN_4^{2-}, the complexity of the system did not allow an interpretation of the observed volume changes in terms of the electrostrictive forces.[11,113,114] Instead, the identification of specific interactions between the solute and the solvent molecules allowed the assignment of the source of the measured volume changes. The expansions for Ru(bpy)CN_4^{2-} in aqueous solutions and in the water pool of reverse micelles have been rationalized in terms of changes in the strength of the CN $\cdots$ HOH bonds. On formation of the ^{3}MLCT state, the hydrogen bonds to the water molecules are expected to be weakened, resulting in an expansion of the solvation sphere. In turn, when the ^{3}MLCT state decays, the opposite effect occurs and a volume contraction of the same magnitude is observed. The same explanation was offered in the case of the supercomplexes between Ru(bpy)-CN_4^{2-} and polyaza macrocycles,[115] taking into account that the changes in strength refer to the CN $\cdots$ HN^+R_2H hydrogen bonds. Also in that case, ^{3}MLCT formation was expected to yield an expansion of the whole macrocycle, while excited-state relaxation was expected to give rise to a contraction of the same magnitude. The values observed were smaller than the expansions for Ru(bpy)CN_4^{2-} in aqueous solution, possibly due to the more rigid second sphere provided by the macrocycles.

The electron-transfer reaction between the metal-to-ligand charge-transfer triplet state of Ru(bpy)$_3^{2+}$ and MV^{2+} was investigated to further examine the thermodynamic basis for the observed volume changes in aqueous solutions in the absence of specific interactions (such as complex formation and/or hydrogen bonds), in view of the hydrophobic nature of the ligand.[12] It was found that in this case, the observed contraction could be explained with the classical Drude–Nernst equation for electrostriction only if a semi-empirical constant is employed instead of the theoretical one.

$$\Delta V_{el} = \frac{(ze)^2}{2r\varepsilon}\frac{\partial \ln \varepsilon}{\partial P} = -\frac{Bz^2}{r} \qquad (31)$$

where B is a constant with a calculated value in water of 4.175 for the radius expressed in Ångströms and the ion charge (z) as an integer. Experimental results have shown that higher B values are needed to explain the partial molar volume of ions in water.[110]

The sensitivity of the measured volume changes in electron-transfer reactions to the environment proves the existence of solute–solvent interactions contributing to the volumetric reaction profile. For instance, the structural volume changes observed for the quenching reaction of excited Ru(bpy)$_3^{2+}$ by various salts of Fe(III) in aqueous solutions strongly depended on the nature of the counterion of the iron salts, due to speciation effects.[100] By using the PAS results together with the formation constants of the several iron complexes present before and after the reaction, the partial molar volumes at high dilution of various species were determined.

The volumetric changes accompanying charge-transfer processes have become an increasingly important parameter capable of characterizing the energetics of the reaction, also due to the expected correlation existing between volume and entropy changes. By determining the enthalpy changes for the charge-transfer process, the entropic term has been determined for some cases in which the Gibbs free energy was independently available.[12,107,108] A linear correlation was found between the structural enthalpy (ΔH_{str}) and volume (ΔV_{str}) changes associated with the formation of the ^{3}MLCT state of the complexes Ru(bpy)$_2$(CN)$_2$ and Ru(bpy)(CN)$_4^{2-}$ in aqueous solutions of 0.1 M monovalent salts.[11] The ΔV_{str} values for these complexes were attributed to photoinduced changes in the hydrogen bond strength between the cyano ligands and the water molecules in the first solvation shell.[99] The linear enthalpy–(structural) volume correlation in aqueous salt solutions was interpreted as arising from an enthalpy–entropy compensation effect induced by the added salt on the hydrogen bond network structure of water. This allowed the determination of the free energy for the formation of the ^{3}MLCT state of each complex.[11] A correlation was also established between the entropy change due to solvent changes and the structural volume change, *i.e.* $T\Delta S_{str} \approx (C_P\rho/\beta)\Delta V_{str}$.

3.2 Electron transfer in photosynthetic reaction centers

Photoacoustic techniques offer extremely interesting possibilities for photosynthesis research. Phenomena that can be easily observed by PAS include the storage of energy by charge separation, oxygen evolution by leaf tissue on the microsecond timescale, and the conformational changes of photosystems caused by charge separation. Investigations on photosynthetic systems using photoacoustic methods have been reviewed recently.[20] Here, we wish to restrict our discussion to the specific aspect of the enthalpic and volumetric changes in the electron-transfer chain. The existence of structural volume changes overlapping the enthalpic changes requires careful separation of the two contributions in order to obtain correct estimates of the energy storage in the electron transport chain. The pioneering work of Arata and Parson demonstrated the usefulness of the photoacoustic method in studies on electron transfer in bacterial reaction centers.[2] Some years later, several works pointed out that the contraction observed in this early investigation developed within the duration of the nanosecond laser pulse.[97,98,116] In oxygenic photosynthetic organisms, the reaction centers of photosystem I (PS I) and photosystem II (PS II) convert the absorbed light energy into stable biochemical products through a number of electron-transfer reactions on different timescales. Thermodynamic properties of these steps have been investigated by pulsed, time-resolved PAS, which was applied both to the primary processes of photosynthesis in the microsecond time window[62,97,98,105–107] and to the terminal charge stabilization on a timescale of milliseconds.[117] The possible complications arising from the coexistence of signals of different origin actually resulted in a potential source of information on the dynamics. In the liquid phase, fast photoacoustic signals are sensitive not only to the enthalpy of

photosynthetic electron-transfer reactions, detected by the thermal expansion of the solution, but also to the large negative volume change of photochemical reaction centers.[2,27,28,97,116,118]

Contractions ranging from −12 to −34 Å^3 have been measured for bacterial reaction centers from *Rhodobacter sphaeroides* associated with the formation of $P^+Q_A^-$.[2,27,97,116] The observed volume change was tentatively assigned to electrostriction and was used to obtain an estimate of the effective dielectric coefficient for the inner matrix of the reaction center.[116] In line with this interpretation, the volume contractions of six bacterial reaction centers containing exchanged quinones ranged from −28 to −42 Å^3 and roughly correlated with the size of the quinone, as expected from electrostriction.[28]

The volume and enthalpy changes for charge transfer in the microsecond timescale in photosynthetic reaction centers of the intact cells of *Synechocystis* PCC 6803 were recently determined.[105] The volume changes for PS I and PS II were determined to be −27 and −2 Å^3, respectively. The energy storage on the 1 μs timescale was estimated to be 80 and 45% per trap in PS I and PS II, respectively. From the free energy of the above reactions as the differences of their redox potentials *in situ*, apparent entropy changes could be estimated as +0.4 and −0.2 eV for PS I and PS II, respectively. These values are similar to those obtained *in vitro* for the purified reaction center complexes on the same timescale.[106,107]

The volume changes in the primary photoreactions of various photosynthetic systems were used to estimate the dielectric coefficient in bacterial reaction centers.[109] To this purpose, an extended form of the Drude–Nernst equation was proposed:

$$\Delta V_{el} = \frac{\partial \Delta G_{el}}{\partial P} = \left(\frac{e^2\kappa}{2\varepsilon}\right)\left(\frac{\partial \ln \varepsilon}{\partial \ln V}\right)\left(\frac{z_+^{\,2}}{r_+} + \frac{z_-^{\,2}}{r_-} + \frac{2z_+z_-}{r_\pm}\right) \quad (32)$$

where ΔV_{el} is the electrostrictive volume change, ΔG_{el} the Born charging energy, P the pressure, z_+ and z_- are the charges on the spherical ions, κ is the compressibility of the protein, V its molar volume, r_+ and r_- the radii of the donor and acceptor, and $r_\pm$ the distance between the ions. The use of this equation and the appropriate choice of parameters allowed essentially all of the available experimental data on bacterial reaction centers to be explained in terms of electrostriction of the separated charges, with small contributions from protein confromational changes. This treatment implied the determination of an effective dielectric constant in the protein matrix of approximately 4.

It is worthwhile to remark upon the substantial improvement in data acquisition which resulted from the use of near infrared light (860 nm) to excite the lowest absorption band of the bacterial reaction centers, allowing the excess energy dissipated as prompt heat, which otherwise gives rise to a useless 'background' signal, to be reduced.[28]

3.3 Volume changes in excited and ground-state proton-transfer reactions

A few reports have appeared dealing with the volume changes observed for proton-transfer reactions in aqueous solutions. Proton-transfer reactions are commonly found in a variety of chemical and biochemical processes, including enzymatic reactions, in which protons can be reagents, products, or intermediates. These reactions are difficult to study since they are generally very fast and not always accompanied by changes in the optical properties of a chromophoric group. The absorbance spectrum of the solvated proton is not known and, therefore, it is impossible to follow the formation of this ionic species optically. One of the attractive features of proton-transfer reactions for the application of photothermal methods is that they often involve a change in the number of charges on going from reactants to products. In most cases, this is known to generate volumetric effects in the solution.[13–15] The observed volume changes for the formation or disappearance of point charges can be partly explained by means of the classical electrostrictive theory,[46] although in many cases empirically determined parameters must be used to quantitatively account for the observed effects.[113]

Time-resolved PAS has been used to study the volume changes accompanying excited-state proton-transfer reactions in aqueous solutions of 2-nitrobenzyl systems[119–123] and aromatic alcohols.[124,125] Proton-transfer reactions from the triplet state of Safranin-T[126] and the ^{3}MLCT of $Ru(bpy)(CN)_4^{2-}$[113] have been also characterized using time-resolved PAS. The technique was able to determine the volumetric changes, contractions in all cases, associated with proton ejection from the reactive state to the solvent, but not the rate of the process, which was below the experimental resolution. Application of faster photothermal techniques is likely to yield information on the dynamics of deprotonation of the strong acid intermediate.[64] By exploiting the pH dependence of the measured contractions it was possible to extract the pK_a of the *aci*-nitro intermediate of some 2-nitrobenzaldehydes[119,120] and of the ^{3}MLCT of $Ru(bpy)(CN)_4^{2-}$.[113] For the latter system, by applying the Drude–Nernst equation for the electrostriction effect with an empirically determined constant to the pH-dependent volume change for the formation of the ^{3}MLCT state, it was possible to obtain a value for the partial absolute molar volume of the hydrated proton in water, $V^0(H^+) = -5.5 \pm 0.8$ cm^3 mol^{-1}.[113] This result is remarkable, since the partial molar volume of ionic species produced in photoreactions cannot always be measured with conventional methods, and extrapolation of values at higher concentration to zero concentration is not always warranted. By using the partial absolute molar volume of the hydrated proton in water, it is now possible, in principle, to estimate the partial molar volumes of the conjugated bases formed on proton ejection from the excited species.

By using photoreleased protons as a source of reactants, ground-state proton-transfer reactions can be characterized as well. For instance, protons released from 2-nitrobenzyl systems can react with hydroxide to give water as a product.[119–121] This reaction occurs with a pH-dependent rate which leads to an apparent lifetime which is accessible by time-resolved PAS at alkaline pH in the range 9–12. Protonation of buffers has also been investigated using pyranine as a proton donor.[125] Neutralization of carboxylates has been studied using 2-nitrobenzaldehyde as a caged proton to induce the ground-state reaction.[127] In all these cases, the bimolecular rate constants of the reactions were determined by carefully choosing the appropriate concentrations of the reactants to obtain apparent reaction rates in the sensitivity range of the technique.

Choi *et al.* measured the enthalpy and the volume changes accompanying photolysis of 2-nitrobenzaldehyde in water using time-resolved TG.[123] From the temporal profile of the grating signal, combined with data from pulsed PAS, volume and enthalpy changes can be determined independently in one particular solvent at a certain temperature and pressure.[90,91] The fast thermal signal is attributed to the thermal grating originating from the photoreaction leading to the formation of the ionic species. The photoproducts are detected as species grating. The photoreleased proton, with a high diffusion coefficient, gives a strong species grating which decays with rate constant of $D_{H^+}q^2$. The positive refractive index change is explained by the volume contraction associated with the presence of the photoreleased proton. The partial molar volume of the proton (−6 to −7 mL mol^{-1}) was determined from the grating intensity, in a similar manner to what was done using time-resolved PAS.[113] From the proton grating intensity, using the molar volume of the proton, the authors estimated the concentration of the photoreleased protons without having to resort to a pH indicator. At high pH, the chemical species responsible for the observed strong and fast-decaying species grating signal was

identified as the hydroxide anion, which reacts with the photo-released protons to form water.

Very recently, the enthalpy and volume changes occurring in the triplet excited-state proton-transfer reactions of safranine-T (SH^+) in aqueous solutions at pH 4.8, 8.3, and 10.4 were investigated using time-resolved PAS and laser flash photolysis.[126] Photoexcitation leads to the prompt formation of the triplet state $^3SH^+$. At pH 4.8 and 10.4, $^3SH^+$ reacts with protons or hydroxy ions to form the dication $^3SH_2^{2+}$ or the neutral ^3S species, with diffusion-controlled rate constants of $k_{H^+} = 1.6 \times 10^{10}$ M^{-1} s^{-1} and $k_{HO^-} = 2.6 \times 10^{10}$ M^{-1} s^{-1}, respectively. From the photoacoustic data the $^3SH^+$ energy was estimated to be 175 kJ mol^{-1}. This value is in good agreement with the thermodynamic data obtained from the acid–base equilibrium. The formation of $^3SH^+$ was accompanied by a volume expansion of 1.8 cm^3 mol^{-1}, which was explained by changes in the hydrogen-bonding interaction of the dye with its solvation sphere. Instead, the volume changes observed upon formation of $^3SH_2^{2+}$ and ^3S accounted for the electrostrictive effect produced by the change in the charge distribution on the dye after the proton-transfer reaction.

3.4 Triplet states and singlet oxygen: volume changes and quantum yields

The characterization of the efficiency of formation and decay rate of triplet states was recognized very early on as one of the problems where photothermal methods could provide useful information.[5] From photoacoustic experiments, it is relatively easy to determine the heat released in the process of triplet formation from the excited singlet state. Depending on the triplet lifetime, the decay may be detectable by either photoacoustic or photorefractive methods. Singlet oxygen photosensitization efficiency can also be studied accurately.

However, even recently, the presence of structural volume changes has been sometimes overlooked as a possible source of systematic errors in the determination of the efficiency. Triplet formation (and decay) can be substantially influenced by concomitant volume changes, due to either electrostriction or specific solute–solvent interactions. Neglecting volume changes results in erroneous estimates of heat release and, hence, quantum yields. The presence of substantial volume changes upon triplet formation and decay has been evidenced for aqueous solutions of porphyrins.[16,103,128] Stronger hydrogen bonding in water in the triplet (and possibly also in the singlet) excited state has been identified as one origin of the structural volume changes for freebase porphyrins.[16,128]

In organic solvents, the contribution to the total signal from structural volume changes is possibly less important. However, structural volume changes are expected to significantly affect the amplitude of the photoacoustic signals in cases where a substantial change in the dipole moment of the molecule or in the number of charges in solution occurs upon photoexcitation.[99,100,103,108,111,112]

In several other systems, the triplet-state formation efficiency was estimated from the photoacoustic signal with no attempt to isolate the contribution from the heat released, thus assuming that volume changes do not represent a significant fraction of the observed signal. These include phthalocyanins,[129] tetrapyridylporphyrins,[130] and merocyanine dyes.[131]

In a series of papers Nonell and co-workers investigated the singlet oxygen sensitization efficiency of a number of triplet sensitizers, also identifying some generally usable standards. The systems they characterized include aromatic ketones,[132] subphthalocyanines,[133] phenalenone,[134] cone-shaped subnaphthalocyanines,[135] neutral and cationic tetrapyridinoporphyrazine,[136] and dihydrofullerene derivatives.[137]

Time-resolved photoacoustics has the advantage of allowing determination of absolute quantum yields, provided the energy of the triplet state is known. This is a major advantage over laser flash photolysis, which always requires a standard to refer to when estimating triplet yields. A similar argument applies for the determination of singlet oxygen yields from near infrared phosphorescence emission. Since the energy of singlet molecular oxygen is known, it is possible to determine the singlet oxygen yield from simple calorimetric calculations.[5,16,138] A comparison between the precision in the obtained parameters using the maximum amplitude and deconvolution methods showed that, when the maximum amplitude method is applicable, it yields equivalent but more precise results.[132]

Using similar methodologies, the triplet yield and the singlet oxygen quantum yield was also determined for tetraphenylporphyrin and its Zn and Cu complexes,[139] as well as for halogenated chlorins.[140]

The photophysical properties of caffeine, theophylline, and theobromine,[141] and their benzophenone-photosensitized reactions in acetonitrile[38] were investigated by time-resolved LIOAS. In the three cases, global quenching rate constants of triplet benzophenone were measured as a function of temperature and it was observed that this is a non-activated process. In addition, heats for NH hydrogen abstraction reactions were determined for theobromine and theophylline. In agreement with semi-empirical calculation predictions, hydrogen abstraction is thermodynamically more favorable and faster for theophylline ($\Delta H = -265$ kJ mol^{-1}, $k_r = 9.6 \times 10^8$ M^{-1} s^{-1}) than for theobromine ($\Delta H = -168$ kJ mol^{-1}, $k_r = 3.7 \times 10^8$ M^{-1} s^{-1}). Also, in this case, the neutral nature of the radicals in the organic solvent allowed contributions from structural volume changes to be neglected.

3.5 Diffusion of reaction intermediates: radicals

In a series of works, Terazima and co-workers have shown the usefulness of the transient grating technique for the measurement of the diffusion coefficients of radicals.[142] Diffusion of intermediates is one of the key factors in controlling chemical reactions and the diffusion coefficient (D) of intermediate species is involved in most of the theories of chemical reactions. Due to the difficulty of measuring D for unstable intermediates as radicals, the diffusion coefficient of a stable molecule with a similar size and shape is used in many cases to analyze the reaction.

In the transient grating method (*vide supra*), two coherent light beams are crossed at a sample to produce the light intensity interference pattern. If a photochemical reaction takes place in a bright region of the grating pattern, the reactants disappear, and intermediate species or products are generated. Since the presence of different chemical species results in a different refractive index and absorbance, photochemical reactions lead to a spatially modulated refractive index or absorbance grating which can be probed with another probe beam, introduced in that region in compliance with the Bragg condition. The grating signal intensity reflects the spatial modulation of the chemical species, becoming weaker as the reactant and the product become spatially uniform in the grating region, which is accomplished by the translational diffusion (or back reaction from the intermediate to the reactant if the reaction is reversible). The diffusion coefficient of the transient species is obtained from the slope of the linear plot of the decay rate constants of the grating signals vs q^2 (the grating wavenumber).[142] This highly sensitive direct method allows short timescale measurements due to the small distances over which diffusion is detected (the fringe spacing) for small volumes of samples and is therefore ideal for unstable radical intermediates. A number of radical reactions have been studied by this method. These include radicals generated by hydrogen abstraction,[143–146] ionic radicals,[147–150] radicals formed by bond dissociation,[146,151,152] radicals from carbenes,[153,154] and some stable radicals.[155]

In general, the radicals created by the hydrogen abstraction reactions were found to diffuse more slowly than the parent molecules with similar volumes. The slower diffusion of the radicals was explained by an attractive intermolecular interaction between the radicals and solvent, occurring at the electronic level. Larger radicals were found to have diffusion coefficients closer to those of the parent molecules.

The temperature dependence of the diffusion coefficients of the radical and the parent molecule for some chemical systems has been investigated in alcoholic solvents.[156,157] The diffusion coefficient can be expressed by an Arrhenius relation:

$$D = D_0 \exp\left(-\frac{E_D}{RT}\right) \qquad (33)$$

It was found that, generally, the activation energies (E_D) for the radicals were smaller than those of the parent molecules. The effect of solvents was also examined[158,159] and it was concluded that D is almost proportional to the inverse of the solvent viscosity, as predicted by the Stokes–Einstein relation. Migration of radicals generated by electron transfer in charged micellar systems has also been investigated, showing the influence of the charge of the micellar surface on the diffusion of the radicals.[160] In the case of stable radicals, the difference between the D of radicals and parent compounds was found to be much smaller than what was observed for transient radicals.[155]

3.6 Protein motions

3.6.1 Biological photoreceptors. Biological photoreceptors are special proteins abundant in all living organisms, from bacteria to plants and mammalians. An organic cofactor is—most often covalently—bound to the protein and provides the capability of absorbing visible light. After light absorption, photochemical reactions of the cofactor take place (the most prominent are photoisomerization and photoinduced electron transfer), leading to structural rearrangements in the protein. The latter enable the photoreceptor to transmit the signal to downstream partner proteins in the signal transduction cascade or act directly in, for example, the regulation of gene expression. Biological photoreceptors have been studied in great detail with PAS, and to a lesser extent by photothermal methods, for two reasons: (i) photoreceptor function is based on the formation of a metastable state (usually on a timescale of seconds or longer), therefore, the estimation of enthalpy content and, possibly, entropic changes is a key issue in order to understand signal transduction; (ii) the photoreaction can be triggered by light and is very often cyclic, *i.e.* can be repeated for the same sample 10^4–10^6 times, with obvious advantages compared to non-photoactive or non-reversible systems.

In the following, we will deal only with the photoreceptors for which the photoisomerization is the primary reaction. For all those photoreceptors [rhodopsin-like, phytochrome, photoactive yellow protein (PYP)], an intermediate state with a photoisomerized chromophore and a protein conformation similar to that of the ground state is formed in a couple of nanoseconds. The stored relative enthalpic energy is high compared to the energy of the excited singlet state (94% in bovine rhodopsin,[161] 61% in octopus rhodopsin,[162] 42% in PYP,[163] 85% in phytochrome,[164] 76% in sensory rhodopsin 1,[165] and 40% in sensory rhodopsin 2[166]) which is, in absolute numbers, 80 to 150 kJ mol^{-1}—more then enough to cross a barrier on the way to the next electronic state. A common interpretation is that the photoinduced isomerization induces a strained chromophore configuration within its protein environment, which is then used to drive protein conformational changes. In a way, the photoisomerization 'stores' the light energy absorbed in metastable states so that the protein conformational changes needed for signal transduction (taking from microseconds to seconds) do not have to compete with the relaxation of the excited states (picoseconds to nanoseconds). It is interesting to note that bacteriorhodopsin and halorhodopsin, two retinal-containing proteins similar to rhodopsin and the sensory rhodopsins, have much less stored energy in the nanosecond intermediate (only *ca.* 15%).[167,168] Neither are photoreceptors, but both still show retinal photoisomerization. They function as ion pumps, namely for protons (bacteriorhodopsin) and chloride (halorhodopsin).

Structural volume changes were found for all photoreaction steps of the different photoreceptors, which were studied by photoacoustic and photothermal methods. It was long thought that those would give a wealth of information about the second key step in photoreceptor action, namely the conformational change of the protein, which is transferred to the downstream partner in the phototransduction signaling pathway. The structural volume changes are expansions or contractions, but of very small magnitude (maximum 100 Å^3, typically < 15 Å^3) compared to that of the protein.[8,10,34,39,77,78,83,161–180] There is also no obvious inter-family correlation between the structural volume change and the function or conformational changes of the photoreceptor. In fact, since the measured structural volume changes are typically of the order of the volume change induced by proton release/uptake, it seems reasonable to assume that the structural volume changes observed are the sum of many different changes in the protein conformation as well as the protonation state of the amino acid side chains. This may efficiently mask the functional protein conformational change. Single-point mutations of crucial amino acids should help to identify the important conformational changes.[181,182] Large differences in structural volume changes, however, have been found for a mutation far away from the chromophore (in PYP[178]) on a timescale where only the chromophore and the surrounding amino acids are believed to be different from the ground state. In the case of sensory rhodopsin 2, enthalpy content and structual volume changes of certain intermediates were influenced by the presence of seven histidines at the C terminus (appended for purification).[166] In other words, the parameters estimated from photothermal methods can be as much influenced by amino acid replacement far away from the photoactive or enzymatic part of the protein as by single-point mutations near these functionally important parts. This can be understood by considering the influential role of the protein dynamics and flexibility—affected by changes in the amino acid composition in all parts of the protein—on the function of a protein. It might, therefore, be misleading to try to obtain information about the function of photoreceptors and enzymes from single-point mutations (see ref. 178), a statement which is more general and not limited to photoacoustic and photothermal methods.

For PYP, a temperature dependence of the structural volume change in pR_1 has been identified by using photoacoustic and thermal grating spectroscopy.[175] This was later interpreted as a change in the thermal expansion coefficient of the protein (in this case a contraction, *i.e.* a larger thermal expansion coefficient) which would reflect structural and entropy fluctuations compared to the ground state. Since the structural volume change is reduced by 50% going from 277 to 298 K it may lead in photoacoustic studies (not only for photoreceptors) to erroneous interpretation of the data and incorrect values for the enthalpies of intermediates and structural volume changes.

An obvious, and long predicted, advantage of photothermal methods is the detection of 'spectrally silent' reaction intermediates, *i.e.* states with identical absorption spectra but different energy contents or configurations/conformations. A number of examples can be found among the chromoproteins, namely bovine rhodopsin [the bathorhodopsin-to-BSI (blue-shifted intermediate) transition],[161] octopus rhodopsin (the transient acid metarhodopsin species and acid metarhodopsin formation[162]), bacteriorhodopsin (K_E intermediate and K_E-to-

K_L transition[77]), and PYP (pR_1 and the pR_1-to-pR_2 transition[178,182]). A closer look, however, reveals that for three of the four cases, clear evidence for the existence of these transitions has been obtained from visible absorption and other spectroscopies (rhodopsin,[181] bacteriorhodopsin,[183,184] and PYP[185,186]). In other words, they are not really 'spectrally silent', but rather just difficult to detect. These three cases have been detected by photoacoustic and transient grating, and their characteristic times lie between 15 ns and 1.5 μs. For bovine rhodopsin, the first, more complicated, reaction scheme was applied to interpret the photoacoustic data, namely an equilibrium between two intermediates.[161] The enthalpies and structural volume changes obtained for two intermediates (BSI and lumirhodopsin) were remarkably different from those which resulted from the use of a simple sequential model.[161,174]

The really interesting conformational changes for the signal transduction are believed to occur 2–4 orders of magnitude slower, and it was hoped to identify those and separate them from the transitions detected by means of TL and PBD. For a number of photoreceptors, the whole photoreaction/photocycle has been studied with the enthalpy stored in the different intermediates always decreasing as the photoreaction proceeds.[78,83,162,177] But, with the exception of octopus rhodopsin (the transient acid metarhodopsin species[162]), no new process characterized by a large enthalpic or entropic change could be identified which was decoupled from the visible absorption changes, the latter reflecting only the chromophore. In fact, it was neccessary and convenient to use the lifetimes obtained from transient absorption changes to fit the photothermal data in order to obtain the amplitudes with higher precision. Even for a photoreceptor (such as PYP) where certain events (like proton uptake and large protein conformational changes) are very precisely assigned to kinetic components of the photocycle studied by visible absorption, no evidence to identify these special processes by means of high enthalpic or entropic changes using photothermal methods could be obtained.[177] In that respect, photothermal methods have not proved as useful as was first thought. The major reason for this is the large contribution of the refractive index changes caused by the absorption changes due to the Kramers–Kronig relation. Its amplitude is often of the order of 80% of the total signal in transient lensing or beam deflection.

3.6.2 Protein folding. Among protein motions, of special interest are protein folding/unfolding reactions. These processes generally involve movements of portions of the protein to allow local interactions between amino acids involved in the secondary structure motifs and global structural rearrangements. The interactions between different amino acids in the polypeptide chain and between amino acid residues and solvent molecules are strongly affected by folding. In the case of pH-dependent equilibria, ionic equilibria are involved as well as ground-state proton-transfer reactions occurring between the solvent and the protein. Volume changes for these reactions are relevant and have been characterized using equilibrium methods (dilatometry and high pressure).[187–193] Therefore, investigation of folding-related protein motions with time-resolved photothermal methods appears to be a promising avenue of research. In order to do so, methods need to be devised to trigger the folding reaction *via* the absorption of light. Recently, 2-nitrobenzaldehyde has been used as a photochemical trigger to initiate ground-state proton-transfer reactions in studies of the dynamics of pH-dependent secondary structures in proteins. Using this method, the rate and the volumetric changes accompanying secondary structure formation in model polypeptides[121,127] and the molten globule formation in apomyoglobin[194] were characterized. The volume change accompanying the neutralization of negatively charged carboxylates, the structural rearrangements of the macromolecule, and the changes in exposure of hydrophobic portions of the molecules are readily detected by time-resolved PAS, without the need for any change in absorption (*i.e.* color). Kinetics from a few tens of nanoseconds to a few microseconds can be deconvoluted from the acoustic signals. This allows monitoring of protein movements which are otherwise elusive to the traditional monitoring methods used in protein folding studies.

It is expected that application of lensing and grating techniques will extend this method to longer timescales, which are of major interest for protein folding problems. For instance, a preliminary work using transient grating showed that kinetics related to acid-induced unfolding of apomyoglobin may be detected on the micro- to millisecond timescale.[122] This study employed 2-nitrobenzaldehyde to induce a fast acidic pH jump in solution and showed that a species grating decaying on the millisecond timescale is due to diffusional motions of the protein. This transient is sensitive to the folding state of the apoprotein, as demonstrated by the effect of urea on the diffusion coefficient.

Transient grating was employed to monitor the changes in global carboxymyoglobin structure as a function of guanidine hydrochloride concentration. The diffusion coefficients of the protein were determined at various concentrations of the denaturant from the time profile of the TG signal after the photodissociation reaction of the ligand. The denaturation curve of carboxymyoglobin monitored through the diffusion coefficient was compared with that monitored by circular dichroism, showing that the global structure of myoglobin undergoes further changes after the secondary structure has relaxed to the denatured state.[195]

3.6.3 Protein dynamics following CO photodissociation. The relationship between structure and function in proteins is of fundamental importance in their characterization and, to this purpose, ligand binding kinetics to myoglobin and hemoglobin has been widely investigated. In these proteins, a small ligand (*e.g.* O_2, CO, NO) is reversibly bound to the sixth coordination site of the Fe-heme, on its distal side. On photoexcitation of the heme, the ligand–metal bond is dissociated. Since there is generally no direct exit to the solvent, the protein structure has to change in order to allow the ligand to escape from the protein.

The structural changes involved in ligand motion through the protein necessarily involve changes in the protein volume, or the development of material strain, *i.e.* the protein has to deform to accommodate the ligand. In this regard, photothermal methods such as PAS[21,31,180,196–199] and TL and TG spectroscopy[9,66,81,179,200–210] provide observables that are sensitive to the global volume changes of the protein and are, therefore, a unique probe of the dynamic coupling between the ligand and protein. Mass displacements show up as changes in the index of refraction of a photoinduced transient lens, changes in the index of refraction or phase component of a photoinduced grating, or changes in pressure.

The dynamics after the photodissociation of carboxymyoglobin has been recently reconsidered in several studies using transient grating[81,203,205,206] and a combination of transient grating and photoacoustics.[207–210]

In horse carboxymyoglobin, a new kinetics was detected, characterized by a 700 ns lifetime at room temperature, which was not observed in flash photolysis experiments.[207,209] This kinetics has been attributed to the relaxation from the geminate pair to the fully dissociated state. The enthalpy of the photodissociated intermediate species was determined to be 61 ± 10 kJ mol^{-1}, which is less than the expected Fe–CO bond energy. The volume of the geminate pair is slightly smaller (ΔV = −5 ± 3 cm^3 mol^{-1}). When CO is released from the protein to the solvent and the protein relaxes to its final state, the volume expands by 14.7 ± 2 cm^3 mol^{-1} at room temperature and 14 ± 10 kJ mol^{-1} is released. The activation parameters for CO escape to the solvent are ΔH^* = 41.3 kJ mol^{-1} and ΔS^* = 13.6 J mol^{-1} K^{-1}. Grating experiments at a high wavenumber

suggested that the volume expansion is temperature dependent. Similar findings were reported for sperm whale carboxymyoglobin.[208] The effect of mutations (H64L, H64Q, H64V) on the CO escape rate was also investigated.[210] The volume change was found to be strongly affected by the nature of the amino acid residue at position 64 in myoglobin. The effect was discussed in terms of heme doming, movement of E and F helices, electrostatic interaction between the bound CO and the distal residue, and movement of the distal water. The main factor determining the amplitude of the volume change was found to be the polarity of the amino acid. It was accordingly suggested that the polar residue at position 64 induces the volume contraction after the photodissociation of CO from the heme because of the disappearance of the repulsive electrostatic interaction between the bound CO and the polar residue 64. The contraction is not observed for the H64L and H64V mutants because the apolar residue at position 64 in these cases has a weak interaction with the bound CO.

Similar findings were reported by Miller and co-workers, who also investigated protein dynamics following CO photodissociation on sub-nanosecond timescale.[9,66,81,201–206] The sensitivity of the transient grating method was recently dramatically improved by the implementation of heterodyne detection of the phase grating signal. This method amplifies the signal-to-noise ratio by more than two orders of magnitude and enables the separation of real (phase) and imaginary (amplitude) parts of the nonlinear, four-wave-mixing diffracted signal. This advance in the spectroscopic method has made it possible to fully resolve ligand escape from the protein in real time. The observation that ligand escape is characterized by a single-exponential decay function provides evidence that is consistent with the view of cavity-directed ligand migration, and it further suggests that there are a very limited number of escape pathways through the protein, with potentially one dominant pathway.

A few other CO complexes have been investigated using time-resolved PAS. The conformational dynamics of ferrous CO–camphor–cytochrome P-450cam, previously investigated by time-resolved PAS,[211] has been recently reconsidered in order to understand the origin of the observed dynamics.[212] Since the Arg186–Asp251–Lys178 bifurcated salt bridge, located above the heme pocket, has been shown to play a key role in the control of the diffusion step of camphor binding, the effects of a site-directed mutation of these linkages and ionic strength increases have been investigated. In this work, the hypothesis that electrostriction resulting from the transient exposure of these charged residues to the solvent could be responsible for part of the photoacoustic signal was tested.

Photolysis of the CO complex of horseradish peroxidase was accompanied by fast volume changes (lifetime below the experimental resolution of the photoacoustic set-up).[213] The volume change (+29.6 mL mol^{-1}) was attributed to the displacement of CO to the bulk solvent. The enthalpy change is mainly related to the Fe–C bond energy with little contribution from the protein matrix. The results were interpreted in terms of the structural properties of horseradish peroxidase, which has a direct exit channel from the heme to the solvent. The reduced expansion and the lower enthalpy change in the photolysis of the related CO complexes of myoglobin and hemoglobin than in horseradish peroxidase both point to additional protein matrix rearrangements, coupled to the photodissociation of CO. These rearrangements give a negative contribution to the volume change, adding algebraically to the volume change due to CO displacement, and an exothermic contribution lowering the reaction enthalpy. This difference was correlated with the absence of a free access channel to the heme in the globins.

Similarly, the volume changes associated with CO photodissociation from fully reduced cytochrome *bo*3 from *Escherichia coli* were studied by time-resolved PAS. Photodissociation was followed by a fast contraction (−5.1 mL mol^{-1}), and a 5 kcal mol^{-1} enthalpy change was estimated for CO binding to Cu_B.[214]

Volume changes associated with CO photodissociation from fully reduced cytochrome *aa*3 have been determined using laser-induced, time-resolved PAS.[215] Two intermediate steps were observed in the photodissociation reaction: a fast, sub-resolution volume change of +6.8 mL mol^{-1} and a 1.5 μs lifetime intermediate associated with an expansion +6.9 mL mol^{-1}. The ΔV for the fast process was attributed to conformational dynamics associated with photoinduced transfer of CO from the high potential heme *a*3 to the high potential Cu_B site, while the timescale of the slower phase was found to be consistent with the thermal dissociation of CO from Cu_B. It was suggested that these volume changes may be linked to movement of Glu242 as part of a proton-shuttle mechanism in heme/copper oxidases.

In order to understand the basis for the volume changes observed in the CO photodissociation and solvation processes in protein reactions, the CO complex with a simple system was considered. Time-resolved photoacustic spectroscopy was used to determine the volume and enthalpy changes for ligand binding associated with CO–Fe(II) protoporphyrin IX solubilized in cetyltrimethylammonium bromide micelles.[216] The enthalpy change associated with this process is 10.4 ± 1.1 kcal mol^{-1}. In addition, the analysis demonstrates that ligand photodissociation results in a volume increase of 3.1 ± 0.3 mL mol^{-1}, which occurs on the 100 ns timescale. In the same vein, volume and enthalpy change were measured for CO association with iron(II) tetrakis(4-sulfonatophenyl)porphyrin [COFe(II)4SP] in aqueous solution. Temperature-dependent PBD was employed to probe the overall enthalpy and volume changes associated with CO photolysis and recombination.[217] Ligand recombination occurred with a pseudo-first-order rate constant of (2.5 ± 0.2) × 10^4 s^{-1} and a corresponding volume decrease of 6 ± 1 mL mol^{-1}. Temperature/pressure-dependent transient absorption spectroscopy was used to determine activation parameters, activation enthalpy (ΔH = 3.9 kcal mol^{-1}), and volume (ΔV = 8.2 mL mol^{-1}) for CO recombination. It was observed that the data are consistent with a mechanism in which photolysis yielded a five-coordinate high spin (H_2O)Fe(II)4SP complex that recombines in a single step to form the low spin CO(H_2O)Fe(II)4SP complex. Coupling photothermal techniques with variable pressure/temperature transient absorption spectroscopy proved to be a powerful approach to probe heme reaction dynamics.

Time-resolved PAS and femtosecond transient absorption were used to characterize the electronic relaxation and ligand-binding reactions that occur following photoexcitation of the (peroxide-to-copper) ligand-to-metal charge-transfer (LMCT) band of oxyhemocyanin from *Limulus polyphemus* and *Busycon canaliculatum.*[218]

3.7 Thermalization processes

Transient grating spectroscopy was recently applied to the study of the thermalization in the back electron-transfer process of the charge-transfer complexes toluene–tetracyanoethylene (TCNE), mesitylene–TCNE, and naphthalene–TCNE in polar liquids. By measuring the population and the acoustic grating signals after the excitation of the charge-transfer band and evaluating the delay time of the first acoustic peak arrival time, an energy-weighted average of the thermalization time of 10 ps was estimated.[219,220]

3.8 Organic photochemistry

Pulsed PAS was first applied as a calorimetric technique to radical processes by Rothberg *et al*. in 1983,[221] who determined the enthalpy of hydrogen abstraction from aniline by triplet benzophenone to form the benzhydrol amine radical pair. The report of Peters *et al.*, introducing deconvolution techniques to

retrieve kinetic and thermodynamic information, followed shortly after.[35] Since then, numerous applications of the method to the study of organic photochemistry have been reported.

Pulsed PAS has been used to determine bond dissociation enthalpies in organic solvents.[222,223] This method has the advantage of being capable of accessing the bond dissociation enthalpy in the solvent and not in the gas phase. One of the experimental challenges is the determination of reaction enthalpies in the presence of changes in the volume occupied by the products compared to reactants. The reaction volume change is only significant when the number of chemical species changes (*i.e.* when the number of bonds broken is not equal to the number of bonds formed) or when large conformational changes occur in more complex molecules, such as proteins.[1,8]

The simultaneous presence of volume changes of enthalpic and structural origin can be handled, in some cases, by measuring the photoacoustic signals in a series of homologous solvents.[40,41] In this way, the two signals can be separated by varying the thermoelastic parameter ($\beta/C_P\rho$) through the series of homologous solvents. Since the photophysics and the photochemistry are generally affected by the different solvents, the quantum yields for the processes under investigation must be determined in each solvent.[223] However, even after this correction, care must be taken to check for possible dependencies of the reaction enthalpies and structural volume changes on the solvent.[47]

The unique ability of this technique to deliver the enthalpy and the structural volume change produced in a particular photoinduced reaction step has made the use of this method to characterize the thermodynamics of photoisomerization processes attractive. Several investigations have dealt with model organic compounds in order to obtain hints concerning the origin of signals observed in photobiological studies. In fact, the application of time-resolved PAS has afforded photophysical and thermodynamic parameters for the production of the first intermediate in aqueous solutions of several biological photoreceptors, such as PYP,[39,170] sensory rhodopsin I,[165] and bovine rhodopsin,[161] all bearing chromophores undergoing *cis–trans* isomerizations as the primary photochemical step.

In several of the investigated model systems, the observed volume changes were relatively small, although much larger than expected for an electrostrictive contraction of the solution. From the data, a picture emerges which relates the photoinduced structural volume changes to the particular type of chromophore–medium interactions.

The photoinduced structural volume changes in aqueous solutions of 3,3'-diethyloxadicarbocyanine iodide (DODCI) were mainly attributed to rearrangement of solvent molecules around the DODCI isomers with different dipole moments.[224] The observed contraction (-29 mL mol^{-1}) upon *trans–cis* isomerization could not be rationalized in terms of the continuum model for electrostriction, for which a contribution of a mere -0.1 mL mol^{-1} was expected. The effect was thus attributed to changes in the hydrogen bond strength between the solvent molecules and the photoisomer *versus* the parent compound. A suggestion was made that the lone pair of one of the heterocyclic nitrogens could be involved in these hydrogen bonds. Similarly, the contractions upon *trans–cis* photoisomerization of the three isomers (*para*, *meta*, and *ortho*) of potassium azobenzenecarboxylates were also rationalized in terms of the difference in the chromophore–water hydrogen bond strength between the photoisomer and the parent compound.[225] In this case, a stronger interaction of the nitrogen lone pairs and water was also suggested for the *cis* isomers, due to reduced conjugation, leading to the contraction upon photoisomerization. Three retinal isomers were also investigated in a series of *n*-alkanes,[226] but the low photoisomerization quantum yield for all-*trans*-retinal and a dependence of the isomerization quantum yield on the solvent for 1,3-*cis*-retinal made quantitative evaluations difficult. To overcome these difficulties, the volume changes associated with photoisomerization were investigated for the water-soluble stilbene derivative 4,4′-dinitro-2,2′-disulfonylstilbene (DS).[227] Taking advantage of the stability of the *cis* and *trans* isomers of DS in their ground states, the volume changes associated with photoisomerization in both directions were determined. Approximately 50% of the observed contractions were attributed to electrostrictive effects. The remaining 50% was assigned to intrinsic effects, related to a shorter C=C bond and a smaller accessible volume in the *cis* isomer.

The involvement of specific solute–solvent interactions in the photoisomerization processes was also suggested for *trans–cis* photoisomerization of azobenzene in ethanol and *p*-coumaric acid in water.[94] For both molecules, ΔV was found to be small and negative. This small volume change has been attributed to the minimal change in the van der Waals volume, solvent-excluding volume, and the dipole moment upon photoisomerization. These findings also indicate that the hydrogen bonding with solvent molecule is not very different for the *cis* and *trans* isomers. These findings lead the authors to conclude that volume changes detected for biological systems using the photoisomerization of *p*-coumaric acid (such as for PYP) should be attributed to the molecular rearrangement of the protein matrix. ΔH values for the *trans–cis* photoisomerization of azobenzene and *p*-coumaric acid were found to be similar.

The structural volume changes upon photoisomerization of bilirubin–albumin complexes for several bilirubins were invariably found to be negligible.[228] This finding was taken as an indication that the part of the molecule undergoing photoisomerization is possibly in a cavity inside the protein, shielded from the aqueous solvent. It was suggested that the interaction between the protein and the chromophore should be loose, due to the absence of detectable structural volume changes.

The formation and deactivation of the pyrene–*N*,*N*-diethylaniline exciplex has been studied in *n*-alkanes by means of time-resolved PAS.[229] The reaction volume of exciplex formation, free of electrostriction contributions, was determined to be -22 cm^3 mol^{-1}. Two principal contributions to the overall reaction volume were ascribed to solvent effects, namely the volume of contact complex formation, and the volume contraction of the solvent around the created dipole. The contribution of bond formation was found to be negligibly small. A direct proportionality between ΔV_{el} and the thermoelastic parameter ($\beta/C_P\rho$) of the solvent was found for *n*-alkanes at 25 °C, suggesting that, thanks to this relationship, reaction volumes and enthalpies determined by time-resolved PAS in the series of *n*-alkanes are generally free of electrostriction contributions. Structural volume changes are directly obtained, overall reaction enthalpies are only obtained after an appropriate correction. This surprising result demonstrates that the electrostriction corrections of PAS results in *n*-alkanes are essentially self-contained in the linearization method generally employed to retrieve volume and enthalpy changes.

The photoconversion of a nitrospiropyrane to its open merocyanine form in a series of aerated cycloalkanes (cyclopentane, cyclohexane, and *cis*- and *trans*-decalin) and of the protonated merocyanine to nitrospiropyrane in aqueous solution were studied by laser-induced optoacoustic spectroscopy.[44]

The primary photochemistry of urocanic acid (UCA), one of the primary UV-absorbing chromophores in the stratum corneum of human skin, has been studied by time-resolved PAS.[230] UCA is formed initially as the *trans* isomer, *t*-UCA. Upon absorption of light, the naturally occurring *t*-UCA isomerizes to the *cis* form, *c*-UCA. Photoacoustic experiments performed on both the *cis* and *trans* isomers reveal the formation of a long-lived intermediate following UV-A excitation, identified as reactive oxygen species produced by the triplet state of UCA.

UCA, is characterized by two electronic transitions in the UV-B, which comprise its broad absorption spectrum and give rise to wavelength-dependent isomerization quantum yields. Using pulsed PAS with laser excitation, it was shown that the wavelength-dependent isomerization yield results from the presence of two distinct, weakly coupled electronic states.[231]

Dissipation of energy in melanins is wavelength dependent, suggesting the existence of different reactivity for the different excited states of the molecule.[232] Using time-resolved PAS, it was found that excitation in the visible range is followed by fast non-radiative relaxation with unitary efficiency. Excitation in the UV is followed by energy storage in a long-lived species which, at 254 nm, accounts for 29% of the absorbed photons. Interaction of natural and synthetic melanins with porphyrins has been studied in solution and in organic matrices by means of several techniques, including photoacoustic spectroscopy.[233,234]

4 Conclusions

Photothermal methods have become mature tools for reliable investigations of photoinitiated events in chemistry and biology. Besides the high sensitivity of the techniques and the huge time range they can access (~1 ps–1 s), they possess unique advantages over other time-resolved methods which render them extremely useful for characterizing photochemical reactions as well as protein dynamics and functions. The kinetics of dark reaction intermediates can be measured provided their formation and decay are accompanied by substantial enthalpic and/or volumetric changes.

Judging from the quantity and the quality of recent works dealing with charge-transfer processes, this appears to be one of the fields where photothermal methods promise to be of greatest use in the characterization of the kinetics and energetics of photoinduced processes. One of the important aspects emerging from electron- and proton-transfer studies is that, in many cases, ground-state reactions can be followed by one of the photothermal methods, depending on their characteristic timescale. The requirement is that the ground-state reactions can be triggered by some photochemical reaction leading to the formation of one of the reactants.

At this stage, the correlation between molecular events and measured volume changes is still in its infancy, but some links to thermodynamic parameters, such as, for example, the correlation between entropy and volume changes, are being currently made. However, the mechanistic interpretation of structural volume changes is sometimes beyond any reasonable hope, due to the complexity of the events being observed. Nevertheless, having access to a generic probe like the volume change may give useful informations on the overall state of the molecule.

Although grating and lensing techniques are inherently more complex, the quality of the kinetic information that can be retrieved, and the time resolution they can achieve under favorable conditions, makes them the most attractive photothermal methods at the moment. However, unlike other photothermal methods, such as time-resolved PAS or transient BD, grating experiments require more sophisticated optics and their implementation is accordingly less straightforward for a standard laser laboratory.

Separation of various contributions to the observed signals is still an issue which requires careful evaluation from case to case. This is especially true for photochemical reactions occurring in organic solvents and for systems where temperature-dependent and/or structural volume changes occur. Attention must be paid also to the refractive index changes originating from the Kramers–Kronig relation, which, in some experimental configurations, may be difficult to separate out.

References

1 J. B. Callis, W. W. Parson and M. Gouterman, Fast changes of enthalpy and volume of flash excitation of *Chromatium* chromatophores, *Biochim. Biophys. Acta*, 1972, **267**, 348–362.
2 H. Arata and W. W. Parson, Enthalpy and volume changes accompanying electron transfer from P-870 to quinones in *Rhodopseudomonas sphaeroides* reaction centers, *Biochim. Biophys. Acta*, 1981, **636**, 70–81.
3 C. K. N. Patel and A. C. Tam, Pulsed optoacoustic spectroscopy of condensed matter, *Rev. Mod. Phys.*, 1981, **53**, 517–550.
4 A. C. Tam, Applications of photoacoustic sensing techniques, *Rev. Mod. Phys.*, 1986, **58**, 381–431.
5 S. E. Braslavsky and G. E. Heibel, Time-resolved photothermal and photoacoustics methods applied to photoinduced processes in solution, *Chem. Rev.*, 1992, **92**, 1381–1410.
6 S. E. Bialkowski, *Photothermal Spectroscopy Methods for Chemical Analysis*, Chemical Analysis Monographs Vol. 134, ed. J. D. Winefordner, John Wiley & Sons, Inc., New York, 1996.
7 D. E. Falvey, Photothermal beam deflection calorimetry in solution photochemistry: recent progress and future prospects, *Photochem. Photobiol.*, 1997, **65**, 4–9.
8 P. J. Schulenberg and S. E. Braslavsky, Time-resolved photothermal studies with biological supramolecules, in *Progress in Photothermal and Photoacoustic Science and Technology*, ed. A. Mandelis and P. Hess, SPIE Press, 1997, ch. 3.
9 R. J. D. Miller, Energetics and dynamics of deterministic protein motion, *Acc. Chem. Res.*, 1994, **27**, 145–150.
10 A. Losi, A. A. Wegener, M. Engelhard and S. E. Braslavsky, Enthalpy-entropy compensation in a photocycle: the K-to-L transition in sensory rhodopsin II from *Natronobacterium pharaonis*, *J. Am. Chem. Soc.*, 2001, **123**, 1766–1767.
11 C. D. Borsarelli and S. E. Braslavsky, Volume changes correlate with enthalpy changes during the photoinduced formation of the ^{3}MLCT state of ruthenium(II) bipyridine cyano complexes in the presence of salts. A case of entropy-enthalpy compensation effect, *J. Phys. Chem. B*, 1998, **102**, 6231–6238.
12 C. D. Borsarelli and S. E. Braslavsky, Enthalpy, volume, and entropy changes associated with the electron transfer reaction between the ^{3}MLCT state of $Ru(Bpy)_3^{2+}$ and methyl viologen cation in aqueous solutions, *J. Phys. Chem. A*, 1999, **103**, 1719–1727.
13 T. Asano and W. J. LeNoble, Activation and reaction volumes in solution, *Chem. Rev.*, 1978, **78**, 407–489.
14 A. Drljaca, C. D. Hubbard, R. vanEldik, T. Asano, M. V. Basilevsky and W. J. leNoble, Activation and reaction volumes in solution. 3, *Chem. Rev.*, 1998, **98**, 2167–2289.
15 R. VanEldik, T. Asano and W. J. LeNoble, Activation and reaction volumes in solution. 2, *Chem. Rev.*, 1989, **89**, 549–688.
16 T. Gensch and S. E. Braslavsky, Volume changes related to triplet formation of water-soluble porphyrins. A laser-induced optoacoustic spectroscopy (LIOAS) study, *J. Phys. Chem. B*, 1997, **101**, 101–108.
17 K. Heihoff, R. W. Redmond, S. E. Braslavsky, M. Rougée, C. Salet, A. Favre and R. V. Bensasson, Quantum yield of triplet and $O_2(^1D_g)$ formation of 4-thiouridine in water and acetonitrile, *Photochem. Photobiol.*, 1990, **51**, 635–641.
18 D. C. Fork and S. K. Herbert, The application of photoacoustic sensing techniques to studies of photosynthesis, *Photochem. Photobiol.*, 1993, **57**, 207–220.
19 S. Malkin and O. Canaani, The uses and characteristics of the photoacoustic method in the study of photosynthesis, *Annu. Rev. Plant Physiol. Plant Mol. Biol.*, 1994, **45**, 493–526.
20 S. K. Herbert, T. Han and T. C. Vogelmann, New applications of photoacoustics to the study of photosynthesis, *Photosynth. Res.*, 2000, **66**, 13–31.
21 K. S. Peters, T. Watson and T. Logan, Photoacoustic calorimetry study of human carboxyhemoglobin, *J. Am. Chem. Soc.*, 1992, **114**, 4276–4278.
22 P. R. Crippa, A. Vecli and C. Viappiani, Time-resolved photoacoustic spectroscopy: new developments of an old idea, *J. Photochem. Photobiol., B*, 1994, **24**, 3–15.
23 T. Gensch, C. Viappiani and S. E. Braslavsky, Laser-induced time-resolved optoacoustic spectroscopy in solution, in *Encyclopedia of Spectroscopy and Spectrometry*, ed. J. C. Lindon, G. E. Tranter, and J. L. Holmes, Academic Press, London, 1999, vol. 2, pp. 1124–1132.
24 L. A. Melton, T. Ni and Q. Lu, Photoacoustic calorimetry: a new cell design and improved analysis algorithms, *Rev. Sci. Instrum.*, 1989, **60**, 3217–3223.
25 L. G. Arnaut, R. A. Caldwell, J. E. Elbert and L. A. Melton, Recent advances in photoacoustic calorimetry: theoretical basis and improvements in experimental design, *Rev. Sci. Instrum.*, 1992, **63**, 5381–5389.

26 O. V. Puchenkov and S. Malkin, Photoacoustic cell for dynamic measurements with nanosecond time resolution, *Rev. Sci. Instrum.*, 1996, **67**, 672–680.
27 O. V. Puchenkov, Z. Kopf and S. Malkin, Photoacoustic diagnostics of laser-induced processes in reaction centers of *Rhodobacter sphaeroides*, *Biochim. Biophys. Acta*, 1995, **1231**, 197–212.
28 G. J. Edens, M. R. Gunner, Q. Xu and D. Mauzerall, The enthalpy and entropy of reaction for formation of $P^+Q_A^-$ from excited reaction centers of *Rhodobacter sphaeroides*, *J. Am. Chem. Soc.*, 2000, **122**, 1479–1485.
29 O. V. Puchenkov, Photoacoustic diagnosis of fast photochemical and photobiological processes. Analysis of inverse problem solution, *Biophys. Chem.*, 1995, **56**, 241–261.
30 G. J. Diebold, Theory of thin layer photoacoustic cells for determination of volume changes in solution, *J. Phys. Chem. B*, 1998, **102**, 5404–5408.
31 K. S. Peters and G. J. Snyder, Time-resolved photoacoustic calorimetry: probing the energetics and dynamics of fast chemical and biochemical reactions, *Science*, 1988, **241**, 1053–1057.
32 S. Abbruzzetti, C. Viappiani, D. H. Murgida, R. Erra-Balsells and G. M. Bilmes, Non toxic, water soluble photocalorimetric reference compounds for UV and visible excitation, *Chem. Phys. Lett.*, 1999, **304**, 167–172.
33 P. J. Schulenberg, M. Rohr, W. Gärtner and S. E. Braslavsky, Photoinduced volume changes associated with the early transformations of bacteriorhodopsin: a laser-induced optoacoustic spectroscopy study, *Biophys. J.*, 1994, **66**, 838–843.
34 S. L. Logunov and M. A. El-Sayed, Redetermination of the quantum yield of photoisomerization and energy content in the K-intermediate of bacteriorhodopsin photocycle and its mutants by the photoacoustic technique, *J. Phys. Chem. B*, 1997, **101**, 6629–6633.
35 J. E. Rudzki, J. L. Goodman and K. S. Peters, Simultaneous determination of photoreaction dynamics and energetics using pulsed, time-resolved photoacoustic calorimetry, *J. Am. Chem. Soc.*, 1985, **107**, 7849–7854.
36 J. R. Small, Deconvolution analysis for pulsed-laser photoacoustics, in *Numerical Computer Methods*, ed. L. Brand and M. L. Johnson, Academic Press, Inc., San Diego, 1992, pp. 505–521.
37 J. R. Small, L. J. Libertini and E. W. Small, Analysis of photoacoustic waveforms using the nonlinear least squares method, *Biophys. Chem.*, 1992, **42**, 24–48.
38 D. H. Murgida, R. E. Balsells, P. R. Crippa and C. Viappiani, Type I photosensitized reactions of oxopurines. Kinetics and thermodynamics of the reaction with triplet benzophenone by time resolved photoacoustics, *Chem. Phys. Lett.*, 1998, **294**, 538–544.
39 T. Gensch, *Zeitaufgeloeste Laser-Induzierte Optoakustische Spektroskopie (LIOAS) an Farbstoffeb, biologischen Photorezeptoren und Photosynthetischen Reaktionszentren in Waessrigen Loesungen*, PhD Thesis, University of Düsseldorf, Germany, 1996.
40 M. S. Herman and J. L. Goodman, Determination of the enthalpy and reaction volume changes of organic photoreactions using photoacoustic calorimetry, *J. Am. Chem. Soc.*, 1989, **111**, 1849–1854.
41 R. R. Hung and J. J. Grabowski, Enthalpy measurements in organic solvents by photoacoustic calorimetry: a solution to the reaction volume problem, *J. Am. Chem. Soc.*, 1992, **114**, 351–353.
42 J. Morais, J. Ma and M. B. Zimmt, Solvent dependence of the twisted excited state energy of tetraphenylethylene: evidence for a zwitterionic state from picosecond optical calorimetry, *J. Phys. Chem.*, 1991, **95**, 3885–3888.
43 J. Morais and M. B. Zimmt, Thermodynamics of intramolecular electron transfer in alkane solvents, *J. Phys. Chem.*, 1995, **99**, 8863–8871.
44 R. M. Williams, G. Klihm and S. E. Braslavsky, Time-resolved thermodynamic profile upon photoexcitation of a nitrospiropyran in cycloalkanes and of the corresponding merocyanine in aqueous solutions, *Helv. Chim. Acta*, 2001, **84**, 2557–2576.
45 E. K. L. Yeow and S. E. Braslavsky, Quenching of zinc tetraphenylporphine by oxygen and by 1,4-benzoquinone in nitrile solvents: An optoacoustic spectroscopy study, *Phys. Chem. Chem. Phys.*, 2002, **4**, 239–247.
46 P. Drude and W. Nernst, Über elektrostriktion durch freie ionen, *Z. Phys. Chem.*, 1894, **15**, 79–85.
47 M. B. Zimmt and P. A. Vath, Separating enthalpy and volume contributions in photothermal experiments: A perspective, *Photochem. Photobiol.*, 1997, **65**, 10–14.
48 R. Schmidt and M. Schütz, Methodical studies on the time resolution of photoacoustic calorimetry, *J. Photochem. Photobiol., A*, 1997, **103**, 39–44.
49 N. S. Foster, S. T. Autrey, J. E. Amonette, J. R. Small and E. W. Small, Laser photoacoustic spectroscopy: A versatile absorption-spectroscopic technique, *Am. Lab.*, 1999, **31**, 96s,98s,100s,102s,104s–106s,108s,14.
50 N. S. Foster, J. E. Amonette, S. T. Autrey and J. T. Ho, Detection of trace levels of water in oil by photoacoustic spectroscopy, *Sens. Actuators, B*, 2001, **77**, 620–624.
51 N. S. Foster, J. E. Amonette and S. T. Autrey, In situ detection of chromate using photoacoustic spectroscopy, *Appl. Spectrosc.*, 1999, **53**, 735–740.
52 B. Schlageter, S. Porting, J. Strassburger, M. C. Moreno Bondi, S. E. Braslavsky, E. Oliveros and A. M. Braun, Development of an optoacoustic sensor module for pH and/or CO_2 determination in aqueous solutions, *Sens. Actuators, B*, 1997, **39**, 443–447.
53 T. Autrey, N. Foster, D. Hopkins and J. Price, Tunable ultraviolet visible photoacoustic detection – Analysis of the sensitivity and selectivity provided by a xenon flash lamp, *Anal. Chim. Acta*, 2001, **434**, 217–222.
54 J. R. Small, N. S. Foster, J. E. Amonette and T. Autrey, Listening to colloidal silica samples: simultaneous measurement of absorbed and scattered light using pulsed-laser photoacoustics, *Appl. Spectrosc.*, 2000, **54**, 1142–1150.
55 T. Autrey, N. Foster and K. Klepzig, Nanojoules, nanoliters and nanosecond calorimetry, *J. Photochem. Photobiol., A*, 1999, **125**, 13–19.
56 J. D. Spear, G. L. Klunder and R. E. Russo, Photothermal deflection spectroscopy of an aqueous sample in a narrow bore quartz capillary, *Rev. Sci. Instrum.*, 1998, **69**, 2259–2267.
57 T. Autrey, N. S. Foster, K. Klepzig, J. E. Amonette and J. L. Daschbach, A new angle into time-resolved photoacoustic spectroscopy: A layered prism cell increases experimental flexibility, *Rev. Sci. Instrum.*, 1998, **69**, 2246–2258.
58 J. A. Daffron, G. J. Farrell and T. J. Burkey, High-pressure photoacoustic calorimetry, *Rev. Sci. Instrum.*, 2000, **71**, 3882–3885.
59 G. J. Farrell and T. J. Burkey, High-pressure photoacoustic calorimetry of chromium hexacarbonyl: volumes of heptane displacement from chromium pentacarbonyl heptane, *J. Photochem. Photobiol., A*, 2000, **137**, 135–139.
60 E. F. Walsh, V. K. Popov, M. W. George and M. Poliakoff, Photoacoustic calorimetry at high pressure: a new approach to determination of bond strengths. Estimation of the M-L bond dissociation energy of $M(CO)_5L$ (M = Cr, Mo; L = H_2, N_2) in n-heptane solution, *J. Phys. Chem.*, 1995, **99**, 12016–12020.
61 E. F. Walsh, M. W. George, S. Goff, S. M. Nikiforov, V. K. Popov, X. Z. Sun and M. Poliakoff, Energetics of the reactions of $(\eta^6\text{-}C_6H_6)Cr(CO)_3$ with n-heptane, N_2, and H_2 studied by high-pressure photoacoustic calorimetry, *J. Phys. Chem.*, 1996, **100**, 19425–19429.
62 L. Nagy, V. Kiss, V. Brumfeld and S. Malkin, Thermal and structural changes of photosynthetic reaction centers characterized by photoacoustic detection with a broad frequency band hydrophone, *Photochem. Photobiol.*, 2001, **74**, 81–87.
63 V. Brumfeld, L. Nagy, V. Kiss and S. Malkin, Wide-frequency hydrophone detection of laser-induced photoacoustic signals in photosynthesis, *Photochem. Photobiol.*, 1999, **70**, 607–615.
64 M. Terazima, Transient lens spectroscopy in a fast timescale, *Isr. J. Chem.*, 1998, **38**, 143–157.
65 M. Terazima, Energy transfer from photoexcited electronic states to the thermal modes, *Bull. Chem. Soc. Jpn.*, 2001, **74**, 595–611.
66 L. Genberg, L. Richard, G. McLendon and R. J. D. Miller, Direct observation of global protein motion in hemoglobin and myoglobin on picosecond time scales, *Science*, 1991, **251**, 1051–1054.
67 E. Vauthey and A. Henseler, Energetics of exciplex formation using picosecond transient thermal phase grating spectroscopy, *J. Phys. Chem.*, 1996, **100**, 170–175.
68 M. Takezaki, N. Hirota and M. Terazima, Nonradiative relaxation processes and electronically excited states of nitrobenzene studied by picosecond time-resolved transient grating method, *J. Phys. Chem. A*, 1997, **101**, 3443–3448.
69 M. Terazima, Photothermal studies of photophysical and photochemical processes by the transient grating method, *Adv. Photochem.*, 1998, **24**, 255–338.
70 M. Terazima, Refractive index change by photothermal effect with a constant density detected as temperature grating in various fluids, *J. Chem. Phys.*, 1996, **104**, 4988–4998.
71 T. Okazaki, N. Hirota and M. Terazima, Picosecond time-resolved transient grating method for heat detection: excited-state dynamics of $FeCl_3$ and *o*-hydroxybenzophenone in aqueous solution, *J. Phys. Chem. A*, 1997, **101**, 650–655.
72 T. Okazaki, N. Hirota, T. Nagata, A. Osuka and M. Terazima, High temporally and spatially resolved thermal energy detection after nonradiative transition in solution using a molecular heater-molecular thermometer integrated system, *J. Am. Chem. Soc.*, 1999, **121**, 5079–5080.

73 T. Okazaki, N. Hirota and M. Terazima, Thermalization process after the relaxation of electronically excited states: Intramolecular proton transfer systems studied by the transient grating method, *J. Chem. Phys.*, 1999, **110**, 11 399–11 410.

74 T. Okazaki, N. Hirota, T. Nagata, A. Osuka and M. Terazima, Spatially resolved thermalization dynamics of electronically photoexcited azulene probed by a molecular integrated thermometer, *J. Phys. Chem. A*, 1999, **103**, 9591–9600.

75 M. Terazima, Vibrational relaxation from electronically photo-excited states in solution studied by the acoustic peak delay method: hydrogen bonding effect to betaine-30, *Chem. Phys. Lett.*, 1999, **305**, 189–196.

76 D. M. Laman and D. E. Falvey, A photothermal beam deflection apparatus for the time-resolved kinetic study of fast photophysical and photochemical processes, *Rev. Sci. Instrum.*, 1996, **67**, 3260–3269.

77 A. Losi, I. Michler, W. Gartner and S. E. Braslavsky, Time-resolved thermodynamic changes photoinduced in 5,12-trans-locked bacteriorhodopsin. Evidence that retinal isomerization is required for protein activation, *Photochem. Photobiol.*, 2000, **72**, 590–597.

78 I. Michler and S. E. Braslavsky, Time-resolved thermodynamic analysis of the oat phytochrome A phototransformation. A photothermal beam deflection study, *Photochem. Photobiol.*, 2001, **74**, 624–635.

79 E. Vauthey, Applicability of the transient grating technique to the investigation of photoinduced processes following second order kinetics, *J. Photochem. Photobiol., A*, 1997, **109**, 195–200.

80 C. Hogemann and E. Vauthey, Picosecond time resolved dispersion spectroscpoy using the interference between population and thermal phase gratings, *Isr. J. Chem.*, 1998, **38**, 181–189.

81 G. Dadusc, G. D. Goodno, H. L. Chiu, J. Ogilvie and R. J. D. Miller, Advances in grating-based photoacoustic spectroscopy for the study of protein dynamics, *Isr. J. Chem.*, 1998, **38**, 191–206.

82 M. Terazima and N. Hirota, Population lens in thermal lens spectroscopy, *J. Phys. Chem.*, 1992, **96**, 7147–7150.

83 P. J. Schulenberg, W. Gärtner and S. E. Braslavsky, Time-resolved volume changes during the bacteriorhodopsin photocycle: a photothermal beam deflection study, *J. Phys. Chem.*, 1995, **99**, 9671–9624.

84 C. Hogemann, M. Pauchard and E. Vauthey, Picosecond transient grating spectroscopy: the nature of the diffracted spectrum, *Rev. Sci. Instrum.*, 1996, **67**, 3449–3453.

85 M. Terazima, Ultrafast transient Kerr lens in solution detected by the dual-beam thermal-lens method, *Opt. Lett.*, 1995, **20**, 25–27.

86 Y. I. Chang, P. Cong and J. D. Simon, Isotropic and anisotropic intermolecular dynamics of liquids studied by femtosecond position-sensitive Kerr lens spectroscopy, *J. Chem. Phys.*, 1997, **106**, 8639–8649.

87 M. Terazima, Ultrafast rise of translational temperature after photoexcitation to electronic excited state in solution: Transient lens study of Ni^{2+} aqueous solution, *J. Chem. Phys.*, 1996, **105**, 6587–6595.

88 M. Terazima, Temperature lens and temperature grating in aqueous solution, *Chem. Phys.*, 1994, **189**, 793–804.

89 M. Terazima and N. Hirota, Rise profile of the thermal lens signal: contribution of the temperature lens and the population lens, *J. Chem. Phys.*, 1994, **100**, 2481–2486.

90 M. Terazima, T. Hara and N. Hirota, Reaction volume and enthalpy changes in photochemical reaction detected by the transient grating method; photodissociation of diphenylcyclopropenone, *Chem. Phys. Lett.*, 1995, **246**, 577–582.

91 T. Hara, N. Hirota and M. Terazima, New application of the transient grating method to a photochemical reaction: the enthalpy, reaction volume change, and partial molar volume measurements, *J. Phys. Chem.*, 1996, **100**, 10 194–10 200.

92 S. Yamaguchi, N. Hirota and M. Terazima, Heat of reaction and reaction volume for the formation of ethers from diazo compounds in methanol, *Chem. Phys. Lett.*, 1998, **286**, 284–290.

93 M. Terazima, Reaction enthalpy and reaction volume changes upon photoenolization: 2-methylbenzophenone, *J. Phys. Chem. A*, 1998, **102**, 545–551.

94 K. Takeshita, N. Hirota and M. Terazima, Enthalpy changes and reaction volumes of photoisomerization reactions in solution: azobenzene and *p*-coumaric acid, *J. Photochem. Photobiol., A*, 2000, **134**, 103–109.

95 O. V. Puchenkov and S. Malkin, On the time resolution of picosecond phase grating spectroscopy in tracing structural relaxation dynamics, *Chem. Phys. Lett.*, 1996, **251**, 242–249.

96 P. A. Vath and M. B. Zimmt, Calibrating picosecond time resolved optical calorimetry: Absolute enthalpies from investigations of mixtures, *Isr. J. Chem.*, 1998, **38**, 207–211.

97 S. Malkin, M. S. Churio, S. Shochat and S. E. Braslavsky, Photochemical energy storage and volume changes in the microsecond time range in bacterial photosynthesis – a laser induced optoacoustic study, *J. Photochem. Photobiol., B*, 1994, **23**, 79–85.

98 I. Yruela, M. S. Churio, T. Gensch, S. E. Braslavsky and A. R. Holzwarth, Optoacoustic and singlet oxygen near-IR emission study of the isolated D1-D2-cyt b-559 reaction center complex of photosystem II. Protein movement associated with charge separation, *J. Phys. Chem.*, 1994, **98**, 12789–12795.

99 J. L. HabibJiwan, B. Wegeweijs, M. T. Indelli, F. Scandola and S. E. Braslavsky, Volume changes associated with intramolecular electron transfer during MLCT state formation. Time-resolved optoacoustic studies of ruthenium cyano complexes, *Recl. Trav. Chim. Pays-Bas*, 1995, **114**, 542–548.

100 C. D. Borsarelli, H. Corti, D. Goldfarb and S. E. Braslavsky, Structural volume changes in photoinduced electron transfer reactions. Laser-induced optoacoustic studies of speciation during the quenching reaction of excited $Ru(bpy)_3^{2+}$ by Fe(III) in aqueous solutions, *J. Phys. Chem. A*, 1997, **101**, 7718–7724.

101 J. Feitelson and D. C. Mauzerall, Wide-band, time-resolved photoacoustic study of electron-transfer reactions: photoexcited magnesium porphyrin and quinones, *J. Phys. Chem.*, 1993, **97**, 8410–8413.

102 D. C. Mauzerall, J. Feitelson and R. Prince, Wide-band time-resolved photoacoustic study of electron transfer reactions: difference between measured enthalpies and redox free energies, *J. Phys. Chem.*, 1995, **99**, 1090–1093.

103 J. Feitelson and D. Mauzerall, Photoacoustic evaluation of volume and entropy changes in energy and electron transfer. Triplet state porphyrin with oxygen and naphthoquinone-2-sulfonate, *J. Phys. Chem.*, 1996, **100**, 7698–7703.

104 K. Sun and D. Mauzerall, Fast photoinduced electron transfer from polyalkyl- to polyfluoro-metalloporphyrins in lipid bilayer membranes, *J. Phys. Chem. B*, 1998, **102**, 6440–6447.

105 V. A. Boichenko, J. M. Hou and D. Mauzerall, Thermodynamics of electron transfer in oxygenic photosynthetic reaction centers: Volume change, enthalpy, and entropy of electron-transfer reactions in the intact cells of the cyanobacterium Synechocystis PCC 6803, *Biochemistry*, 2001, **40**, 7126–7132.

106 J. Hou, V. A. Boichenko, Y. Wang, P. R. Chitnis and D. Mauzerall, Thermodynamics of electron transfer in oxygenic photosynthetic reaction centers: a pulsed photoacoustic study of electron transfer in photosystem I reveals a similarity to bacterial reaction centers in both volume change and entropy, *Biochemistry*, 2001, **40**, 7109–7116.

107 J. M. Hou, V. A. Boichenko, B. A. Diner and D. Mauzerall, Thermodynamics of electron transfer in oxygenic photosynthetic reaction centers: volume change, enthalpy, and entropy of electron-transfer reactions in manganese-depleted photosystem II core complexes, *Biochemistry*, 2001, **40**, 7117–7125.

108 J. Feitelson and D. Mauzerall, Enthalpy and electrostriction in the electron-transfer reaction between triplet zinc uroporphyrin and ferricyanide, *J. Phys. Chem. B*, 2002, **106**, 9674–9678.

109 D. Mauzerall, J. M. Hou and V. A. Boichenko, Volume changes and electrostriction in the primary photoreactions of various photosynthetic systems: estimation of dielectric coefficient in bacterial reaction centers and of the observed volume changes with the Drude-Nernst equation, *Photosynth. Res.*, 2002, **74**, 173–180.

110 F. J. Millero, The molal volumes of electrolytes, *Chem. Rev.*, 1971, **71**, 147–176.

111 B. Wegewijs, J. W. Verhoeven and S. E. Braslavsky, Volume changes associated with intramolecular exciplex formation in a semiflexible donor-bridge-acceptor compound, *J. Phys. Chem.*, 1996, **100**, 8890–8894.

112 B. Wegewijs, M. N. Paddon-Row and S. E. Braslavsky, Volume change associated with large photoinduced dipole formation in a rigid donor-acceptor compound: new approach to optoacoustic volume determination, *J. Phys. Chem. A*, 1998, **102**, 8812–8818.

113 C. D. Borsarelli and S. E. Braslavsky, The partial molar volume of the proton in water determined by laser-induced optoacoustic studies, *J. Photochem. Photobiol., B*, 1998, **43**, 222–228.

114 C. D. Borsarelli and S. E. Braslavsky, Nature of the water structure inside the pools of reverse micelles sensed by laser-induced optoacoustic spectroscopy, *J. Phys. Chem. B*, 1997, **101**, 6036–6035.

115 C. D. Borsarelli, S. E. Braslavsky, M. T. Indelli and F. Scandola, Photophysics of supercomplexes. A laser-induced optoacoustic study of the adducts between $Ru(bpy)(CN)_4^{2-}$ and polyaza macrocycles, *Chem. Phys. Lett.*, 2000, **317**, 53–58.

116 D. C. Mauzerall, M. R. Gunner and J. W. Zhang, Volume contraction on photoexcitation of the reaction center from *Rhodobacter spaeroides* R-26: internal probe of dielectrics, *Biophys. J.*, 1995, **68**, 275–280.

117 D. Charlebois and D. Mauzerall, Energy storage and optical cross-section of PS I in the cyanobacterium Synechococcus PCC 7002 and a psaE$^-$ mutant, *Photosynth. Res.*, 1999, **59**, 27–38.

118 R. Delosme, G. Olive and F. A. Wollman, Changes in light energy distribution upn state transition: an in vivo photoacoustic study of the wild type and photosynthesis mutants from *Chlamydomonas Reinhardtii*, *Biochim. Biophys. Acta*, 1996, **1273**, 150–158.

119 G. Bonetti, A. Vecli and C. Viappiani, Reaction volume of water formation detected by time resolved photoacoustics: photoinduced proton transfer between *o*-nitrobenzaldehyde and hydroxyls in water, *Chem. Phys. Lett.*, 1997, **269**, 268–273.

120 M. Carcelli, P. Pelagatti and C. Viappiani, Determination of the pK_a of the *aci*-nitro intermediate in *o*-nitrobenzyl systems, *Isr. J. Chem.*, 1998, **38**, 213–221.

121 C. Viappiani, S. Abbruzzetti, J. R. Small, L. J. Libertini and E. W. Small, An experimental methodology for measuring volume changes in proton transfer reactions in aqueous solutions, *Biophys. Chem.*, 1998, **73**, 13–22.

122 J. Choi, N. Hirota and M. Terazima, Enthalpy and volume changes on the pH jump process studied by the transient grating technique, *Anal. Sci.*, 2001, **17**, s13–s15.

123 J. Choi, N. Hirota and M. Terazima, A pH-jump reaction studied by the transient grating method: photodissociation of o-nitro-benzaldehyde, *J. Phys. Chem. A*, 2001, **105**, 12–18.

124 A. Losi and C. Viappiani, Reaction volume and rate constants for the excited state proton transfer in aqueous solutions of naphthols, *Chem. Phys. Lett.*, 1998, **289**, 500–506.

125 J. R. Small and E. Kurian, Volumetric photoacoustics: listening to more than just heat, *Spectroscopy*, 1995, **10**, 27–33.

126 C. D. Borsarelli, S. G. Bertolotti and C. M. Previtali, Thermodynamic changes in the photoinduced proton-transfer reaction of the triplet state of safranine-T, *Photochem. Photobiol. Sci.*, 2002, **1**, 574–580.

127 S. Abbruzzetti, C. Viappiani, J. R. Small, L. J. Libertini and E. W. Small, Kinetics of local helix formation in poly-L-glutamic acid studied by time-resolved photoacoustics: neutralization reactions of carboxylates in aqueous solutions and their relevance to the problem of protein folding, *Biophys. J.*, 2000, **79**, 2714–2721.

128 T. Gensch, C. Viappiani and S. E. Braslavsky, Structural volume changes upon photoexcitation of porphyrins: role of the nitrogen – water interactions, *J. Am. Chem. Soc.*, 1999, **121**, 10573–10582.

129 D. Frackowiak, A. Planner, A. Waszkowiak, A. Boguta, R. M. Ion and K. Wiktorowicz, Yield of intersystem (singlet-triplet) crossing in phthalocyanines evaluated on the basis of a time in resolved photothermal method, *J. Photochem. Photobiol., A*, 2001, **141**, 101–108.

130 D. J. Qian, A. Planner, J. Miyake and D. Frackowiak, Photothermal effects and fluorescence spectra of tetrapyridylporphyrins, *J. Photochem. Photobiol., A*, 2001, **144**, 93–99.

131 A. Planner and D. Frackowiak, Fast and slow processes of thermal deactivation of excited stilbazolium merocyanine dyes, *J. Photochem. Photobiol., A*, 2001, **140**, 223–228.

132 C. Marti, O. Jürgens, O. Cuenca, M. Casals and S. Nonell, Aromatic ketones as standards for singlet molecular oxygen $O_2(^1\Delta_g)$ photosensitization. Time-resolved photoacoustic and near-IR emission studies, *J. Photochem. Photobiol., A*, 1996, **97**, 11–18.

133 B. D. Rey, U. Keller, T. Torres, G. Rojo, F. Agulló-López, S. Nonell, C. Martí, S. Brasselet, I. Ledoux and J. Zyss, Synthesis, nonlinear optical, photophysical and electrochemical properties of subphthalocyanines, *J. Am. Chem. Soc.*, 1998, **120**, 12808–12817.

134 E. Oliveros, S. H. Bossmann, S. Nonell, C. Martí, G. Heit, G. Tröscher, A. Neuner and A. M. Braun, The photochemistry of the singlet oxygen ($O_2(^1\Delta_g)$) sensitizer perinaphthenone (phenalenone) in N,N′-dimethylacetamide and 1,4-dioxane, *New J. Chem.*, 1999, **23**, 85–93.

135 S. Nonell, N. Rubio, B. D. Rey and T. Torres, Synthesis, optical absorption and photophysical properties of cone-shaped subnaphthalocyanine, *J. Chem. Soc., Perkin Trans. 2*, 2000, 1091–1094.

136 C. Martí, S. Nonell, M. Nicolau and T. Torres, Photophysical properties of neutral and cationic tetrapyridino-porphyrazines, *Photochem. Photobiol.*, 2000, **71**, 53–59.

137 F. Prat, C. Martí, S. Nonell, X. Zhang, C. S. Foote, R. González Moreno and J. L. Bourdelande, C_{60} fullerene-based materials as singlet oxygen $O_2(^1\Delta_g)$ photosensitizers: a time-resolved near-IR luminescence and optoacoustic study, *Phys. Chem. Chem. Phys.*, 2001, **3**, 1638–1643.

138 A. Losi, R. Bedotti and C. Viappiani, Time-resolved photoacoustics determination of intersystem crossing and singlet oxygen photosensitization quantum yields for 4,5′,8-trimethylpsoralen in various solvents, *J. Phys. Chem.*, 1995, **99**, 16 162–16 167.

139 M. Pineiro, A. L. Carvalho, M. M. Pereira, A. M. D. A. RochaGonsalves, L. G. Arnaut and S. J. Formosinho, Photoacoustic measurements of porphyrin triplet state quantum yields and singlet-oxygen efficiences, *Chem. Eur. J.*, 1998, **4**, 2299–2307.

140 M. Pineiro, M. M. Pereira, A. Gonsalves, L. G. Arnaut and S. J. Formosinho, Singlet oxygen quantum yields from halogenated chlorins: potential new photodynamic therapy agents, *J. Photochem. Photobiol., A*, 2001, **138**, 147–157.

141 D. H. Murgida, G. M. Bilmes and R. Erra Balsells, A photophysical study of purines and theophylline by using laser-induced optoacoustic spectroscopy, *Photochem. Photobiol.*, 1996, **64**, 777–784.

142 M. Terazima, Is the translational diffusion of organic radicals different from that of closed-shell molecules?, *Acc. Chem. Res.*, 2000, **33**, 687–694 and references therein.

143 M. Terazima and N. Hirota, Translational diffusion of a transient radical studied by the transient grating method; pyrazinyl radical in 2-propanol, *J. Chem. Phys.*, 1993, **98**, 6257–6262.

144 M. Terazima, K. Okamoto and N. Hirota, Translational diffusion of transient radicals created by the photo-induced hydrogen abstraction reaction in solution; Anomalous size dependence in the radical diffusion, *J. Chem. Phys.*, 1995, **102**, 2506–2515.

145 K. Okamoto, N. Hirota and M. Terazima, Comments on "Diffusion of free radicals in solution. TEMPO, diphenyl-picrylhydrazyl, and nitrosodisulfonate", *J. Phys. Chem.*, 1997, **101**, 5380–5381.

146 A. Ukai, N. Hirota and M. Terazima, Radical diffusion measured by the transient grating in a short timescale, *Chem. Phys. Lett.*, 2000, **319**, 427–433.

147 M. Terazima, T. Okazaki and N. Hirota, Translational diffusion process of charged radical; TMPD and its cation radical, *J. Photochem. Photobiol., A*, 1995, **92**, 7–12.

148 T. Okazaki, N. Hirota and M. Terazima, Dynamics of aggregate formation and translational diffusion of a spiropyran studied by the transient grating method, *J. Photochem. Photobiol.*, 1996, **99**, 155–163.

149 M. Terazima, Optical heterodyne detected transient grating for the separations of phase and amplitude gratings and of different chemical species, *J. Phys. Chem. A*, 1999, **103**, 7401–7407.

150 K. Okamoto, N. Hirota and M. Terazima, Diffusion of electrically neutral radicals and anion radicals created by photochemical reactions, *J. Chem. Soc., Faraday Trans.*, 1998, **94**, 185–194.

151 M. Terazima, Y. Nogami and T. Tominaga, Diffusion of a radical from an initiator of a free radical polymerization: a radical from AIBN, *Chem. Phys. Lett.*, 2000, **332**, 503–507.

152 K. Okamoto, N. Hirota and M. Terazima, Diffusion process of the benzyl radical created by photodissociation probed by the transient grating method, *J. Phys. Chem. A*, 1997, **101**, 5269–5277.

153 M. Terazima, H. Tomioka, K. Hirai, Y. Tanimoto, Y. Fujiwara and Y. Akimoto, Translational diffusion of a carbene and radicals derived from carbene, *J. Chem. Soc., Faraday Trans.*, 1996, **92**, 2361–2368.

154 M. Terazima, K. Hirai and H. Tomioka, Translational diffusion of chemically active species: carbenes and carbonyl oxides, *Chem. Phys. Lett.*, 1998, **289**, 253–260.

155 M. Terazima, S. Tenma, H. Watanabe and T. Tominaga, Translational diffusion of chemically stable and reactive radicals in solution, *J. Chem. Soc., Faraday Trans.*, 1996, **92**, 3057–3062.

156 M. Terazima, K. Okamoto and N. Hirota, Translational diffusion of transient radicals studied by the transient grating method, *J. Mol. Liq.*, 1995, **65–66**, 401–404.

157 K. Okamoto, M. Terazima and N. Hirota, Temperature dependence of diffusion of radical intermediates probed by the transient grating method, *J. Chem. Phys.*, 1995, **103**, 10 445–10 452.

158 Y. Kimura, D. Kanda, M. Terazima and N. Hirota, Solvent density dependence of translational diffusion of transient radicals in the medium-density region of trifluoromethane and carbon dioxide, *J. Phys. Chem.*, 1997, **101**, 4442–4447.

159 K. Okamoto, N. Hirota and M. Terazima, Diffusion of photochemically generated intermediate radicals in water-ethanol mixed solvents, *J. Phys. Chem. A*, 1998, **102**, 3447–3454.

160 K. Okamoto, N. Hirota, T. Tominaga and M. Terazima, Translational diffusion of ion radicals created by electron transfer in charged micellar solutions probed by the transient grating method and the Taylor dispersion method, *J. Phys. Chem. A*, 2001, **105**, 6586–6593.

161 T. Gensch, J. M. Strassburger, W. Gartner and S. E. Braslavsky, Volume and enthalpy changes upon photoexcitation of bovine rhodopsin derived from optoacoustic studies by using an equilibrium between bathorhodopsin and blue-shifted intermediate, *Isr. J. Chem.*, 1998, **38**, 231–236.

162 Y. Nishioku, M. Nakagawa, M. Tsuda and M. Terazima, Energetics and volume changes of the intermediates in the photolysis of octopus rhodopsin at a physiological temperature, *Biophys. J.*, 2002, **83**, 1136–1146.

163 M. E. VanBrederode, T. Gensch, W. D. Hoff, K. J. Hellingwerf and S. E. Braslavsky, Photoinduced volume change and energy storage associated with the early transformations of the photoactive yellow protein from *Ectothiorhodospira halophila*, *Biophys. J.*, 1995, **68**, 1101–1109.

164 T. Gensch, M. S. Churio, S. E. Braslavsky and K. S. Schaffner, Primary quantum yield and volume change of phytochrome-A phototransformation determined by laser-induced optoacoustic spectroscopy (LIOAS), *Photochem. Photobiol.*, 1996, **63**, 719–725.

165 A. Losi, S. E. Braslavsky, W. Gartner and J. L. Spudich, Time-resolved absorption and photothermal measurements with sensory rhodopsin I from Halobacterium salinarum, *Biophys. J.*, 1999, **76**, 2183–2191.

166 A. Losi, A. A. Wegener, M. Engelhard, W. Gartner and S. E. Braslavsky, Time-resolved absorption and photothermal measurements with recombinant sensory rhodopsin II from Natronobacterium pharaonis, *Biophys. J.*, 1999, **77**, 3277–86.

167 D. Zhang and D. Mauzerall, Volume and enthalpy changes in the early steps of bacteriorhodopsin photocycle studied by time-resolved photoacoustics, *Biophys. J.*, 1996, **71**, 381–388.

168 A. Losi, A. A. Wegener, M. Engelhard and S. E. Braslavsky, Thermodynamics of the early steps in the photocycle of Natronobacterium pharaonis halorhodopsin. Influence of medium and of anion substitution, *Photochem. Photobiol.*, 2001, **74**, 495–503.

169 A. Losi, E. Polverini, B. Quest and W. Gaertner, First evidence for phototropin-related blue-light receptors in prokaryotes, *Biophys. J.*, 2002, **82**, 2627–2634.

170 T. Gensch, K. J. Hellingwerf, S. E. Braslavsky and K. Schaffner, Photoequilibrium in the primary steps of the photoreceptors phytochrome A and photoactive yellow protein, *J. Phys. Chem. A*, 1998, **102**, 5398–5405.

171 A. Losi, A. A. Wegener, M. Engelhard, W. Gartner and S. E. Braslavsky, Aspartate 75 mutation in sensory rhodopsin II from Natronobacterium pharaonis does not influence the production of the K-like intermediate, but strongly affects its relaxation pathway, *Biophys. J.*, 2000, **78**, 2581–2589.

172 Y. Nishioku, N. Hirota, M. Nakagawa, M. Tsuda and M. Terazima, The energy and dynamics of photoreaction intermediates of octopus rhodopsin studied by the transient grating method, *Anal. Sci.*, 2001, **17**, S323–S325.

173 Y. Nishioku, M. Nakagawa, T. M. Tsuda and M. Terazima, A spectrally silent transformation in the photolysis of octopus rhodopsin: a protein conformational change without any accompanying change of the chromophore's absorption, *Biophys. J.*, 2001, **80**, 2922–2927.

174 J. M. Strassburger, W. Gartner and S. E. Braslavsky, Volume and enthalpy changes after photoexcitation of bovine rhodopsin: laser-induced optoacoustic studies, *Biophys. J.*, 1997, **72**, 2294–2303.

175 K. Takeshita, N. Hirota, Y. Imamoto, M. Kataoka, F. Tokunaga and M. Terazima, Temperature-dependent volume change of the initial step of the photoreaction of photoactive yellow protein (PYP) studied by transient grating, *J. Am. Chem. Soc.*, 2000, **122**, 8524–8528.

176 K. Takeshita, N. Hirota, Y. Imamoto, M. Kataoka, F. Tokunaga and M. Terazima, The structural change and energy dynamics in the photocycle of photoactive yellow protein (PYP), *Anal. Sci.*, 2001, **17**, S320–S322.

177 K. Takeshita, Y. Imamoto, M. Kataoka, F. Tokunaga and M. Terazima, Themodynamic and transport properties of intermediate states of the photocyclic reaction of photoactive yellow protein, *Biochemistry*, 2002, **41**, 3037–3048.

178 K. Takeshita, Y. Imamoto, M. Kataoka, K. Mihara, F. Tokunaga and M. Terazima, Structural change of site-directed mutants of PYP: New dynamics during pR state, *Biophys. J.*, 2002, **83**, 1567–1577.

179 M. Terazima, Protein dynamics detected by the time-resolved transient grating technique, *Pure Appl. Chem.*, 2001, **73**, 513–517.

180 K. S. Peters, T. Watson and K. Marr, Time-resolved photoacoustic calorimetry: a study of myoglobin and rhodopsin, *Annu. Rev. Biophys. Biophys. Chem.*, 1991, **20**, 343–362.

181 S. J. Hug, J. W. Lewis, C. M. Einterz, T. E. Thorgeirsson and D. S. Kliger, Nanosecond photolysis of rhodopsin – Evidence for a new, blue-shifted Intermediate, *Biochemistry*, 1990, **29**, 1475–1485.

182 T. Gensch, A. Losi, J. Hendriks, K. J. Hellingwerf and S. E. Braslavsky, manuscript in preparation.

183 A. K. Dioumaev and M. S. Braiman, Two bathointermediates of the bacteriorhodopsin photocycle, distinguished by nanosecond time-resolved FTIR spectroscopy at room temperature, *J. Phys. Chem. B*, 1997, **101**, 1655–1662.

184 W. Hage, M. Kim, H. Frei and R. A. Mathies, Protein dynamics in the bacteriorhodopsin photocycle: a nanosecond step-scan FTIR investigation of the KL to L transition, *J. Phys. Chem.*, 1996, **100**, 16026–16033.

185 E. Chen, T. Gensch, A. B. Gross, J. Hendriks, K. J. Hellingwerf and D. S. Kliger, Dynamics of protein and chromophore structural changes in the photocycle of photoactive yellow protein monitored by time-resolved optical rotary dispersion, *Biochemistry*, 2003, **42**, 2062–2071.

186 K. J. Hellingwerf, J. Hendriks and T. Gensch, Photoactive yellow protein, a new type of photoreceptor protein: will this "yellow lab" bring us where we want to go?, *J. Phys. Chem. A*, 2003, **107**, 1082–1094.

187 J. Rasper and W. Kauzmann, Volume changes in protein reactions. I. Ionization reactions of proteins, *J. Am. Chem. Soc.*, 1962, **84**, 1771–1777.

188 J. Rasper and W. Kauzmann, Volume changes in protein reactions. II. Comparison of ionization reactions in proteins and small molecules, *J. Am. Chem. Soc.*, 1962, **84**, 1777–1788.

189 M. Gross and R. Jaenicke, Proteins under pressure. The influence of high pressure on structure, function and assembly of proteins and protein complexes, *Eur. J. Biochem.*, 1994, **221**, 617–630.

190 T. V. Chalikian, V. S. Gindikin and K. J. Breslauer, Volumetric characterization of the native, molten globule and unfolded states of cytochrome c at acidic pH, *J. Mol. Biol.*, 1995, **250**, 291–306.

191 T. V. Chalikian, On volume changes accompanying conformational transitions of biopolymers, *Biopolymers*, 1996, **39**, 619–626.

192 G. J. A. Vidugiris and C. A. Royer, Determination of the volume changes for pressure-induced transitions of apomyoglobin between the native, molten globule, and unfolded states, *Biophys. J.*, 1998, **75**, 463–470.

193 C. A. Royer, Revisiting volume changes in pressure-induced protein unfolding, *Biochim. Biophys. Acta*, 2002, **1595**, 201–209.

194 S. Abbruzzetti, E. Crema, L. Masino, A. Vecli, C. Viappiani, J. R. Small, L. J. Libertini and E. W. Small, Fast events in protein folding. Structural volume changes accompanying the early events in the N->I transition of apomyoglobin induced by ultrafast pH jump, *Biophys. J.*, 2000, **78**, 405–415.

195 J. Choi and M. Terazima, Denaturation of a protein monitored by diffusion coefficients: Myoglobin, *J. Phys. Chem. B*, 2002, **106**, 6587–6593.

196 J. A. Westrick, J. L. Goodman and K. S. Peters, A time-resolved photoacoustic calorimetry study of the dynamics of enthalpy and volume changes produced in the photodissociation of carbon monoxide from sperm whale carboxymyoglobin, *Biochemistry*, 1987, **26**, 8313–8318.

197 J. A. Westrick, K. S. Peters, J. D. Ropp and S. G. Sligar, Role of the arginine-45 salt bridge in ligand dissociation from sperm whale carboxymyoglobin as probed by photoacoustic calorimetry, *Biochemistry*, 1990, **29**, 6741–6746.

198 J. A. Westrick and K. S. Peters, A photoacoustic calorimetric study of horse myoglobin, *Biophys. Chem.*, 1990, **37**, 73–79.

199 C. L. Norris and K. S. Peters, A photoacoustic calorimetry study of horse carboxymyoglobin on the 10-nanosecond time scale, *Biophys. J.*, 1993, **65**, 1660–1665.

200 G. D. Goodno, G. Dadusc and R. J. D. Miller, Ultrafast heterodyne-detected transient-grating spectroscopy using diffractive optics, *J. Opt. Soc. Am. B*, 1998, **15**, 1791–1794.

201 J. Deak, H. L. Chiu, C. M. Lewis and R. J. D. Miller, Ultrafast phase grating studies of heme proteins: observation of the low-frequency modes directing functionally important protein motions, *J. Phys. Chem. B*, 1998, **106**, 6621–6634.

202 G. D. Goodno and R. J. D. Miller, Femtosecond heterodyne-detected four-wave-mixing studies of deterministic protein motions. 1. Theory and experimental technique of diffractive optics-based spectroscopy, *J. Phys. Chem. A*, 1999, **103**, 10619–10629.

203 G. D. Goodno and R. J. D. Miller, Femtosecond heterodyne-detected four-wave-mixing studies of deterministic protein motions. 2. Protein response, *J. Phys. Chem. A*, 1999, **103**, 10630–10643.

204 G. D. Goodno, V. Astinov and R. J. D. Miller, Diffractive optics-based heterodyne-detected grating spectroscopy: application to ultrafast protein dynamics, *J. Phys. Chem. B*, 1999, **103**, 603–607.

205 G. Dadusc, J. P. Ogilvie, P. Schulenberg, U. Marvet and R. J. D. Miller, Diffractive optics-based heterodyne-detected four-wave mixing signals of protein motion: From "protein quakes" to ligand escape for myoglobin, *Proc. Natl. Acad. Sci. U. S. A.*, 2001, **98**, 6110–6115.

206 J. P. Ogilvie, M. Plazanet, G. Dadusc and R. J. D. Miller, Dynamics of ligand escape in myoglobin: Q-band transient absorption and four-wave mixing studies, *J. Phys. Chem. B*, 2002, **106**, 10460–10467.

207 M. Sakakura, N. Hirota, K. Konishi, I. Morishima and M. Terazima, Study on photodissociation of carboxymyoglobin by the transient grating and photoacoustic methods, *Anal. Sci.*, 2001, **17**, S317–S319.

208 M. Sakakura, I. Morishima and M. Terazima, The structural dynamics and ligand releasing process after the photodissociation of sperm whale carboxymyoglobin, *J. Phys. Chem. B*, 2001, **105**, 10424–10434.

209 M. Sakakura, S. Yamaguchi, N. Hirota and M. Terazima, Dynamics of structure and energy of horse carboxymyoglobin after photodissociation of carbon monoxide, *J. Am. Chem. Soc.*, 2001, **123**, 4286–4294.

210 M. Sakakura, I. Morishima and M. Terazima, Structural dynamics of distal histidine replaced mutants of myoglobin accompanied with the photodissociation reaction of the ligand, *Biochemistry*, 2002, **41**, 4837–4846.

211 C. DiPrimo, G. H. BonHoa, H. Deprez, P. Douzou and S. G. Sligar, Conformational dynamics of cytochrome P-450cam as monitored by photoacoustic calorimetry, *Biochemistry*, 1993, **32**, 3671–3676.

212 C. DiPrimo, E. Deprez, S. G. Sligar and G. H. B. Hoa, Origin of the photoacoustic signal in cytochrome P-450cam: role of the Arg186-Asp251-Lys178 bifurcated salt bridge, *Biochemistry*, 1997, **36**, 112–118.

213 A. Feis and L. Angeloni, Photodissociation of the CO complex of horseradish peroxidase studied by laser-induced optoacoustic spectroscopy, *J. Phys. Chem. B*, 2001, **105**, 2638–2643.

214 R. W. Larsen, J. Osborne, T. Langley and R. B. Gennis, Volume changes associated with CO photodissociation from fully reduced cytochrome *bo*3 from Escherichia coli, *J. Am. Chem. Soc.*, 1998, **120**, 8887–8888.

215 R. W. Larsen and T. Langley, Volume changes associated with CO photolysis from fully reduced bovine heart cytochrome aa(3), *J. Am. Chem. Soc.*, 1999, **121**, 4495–4499.

216 R. W. Larsen, Volume and thermodynamic profiles of CO-binding to Fe(II) protoporphyrin IX in detergent micelles, *Inorg. Chim. Acta*, 1999, **288**, 74–81.

217 B. D. Barker and R. W. Larsen, Volume and enthalpy profiles of CO binding to Fe(II) tetrakis-(4-sulfonatophenyl)porphyrin, *J. Inorg. Biochem.*, 2001, **85**, 107–116.

218 J. S. Floyd, N. Haralampus-Grynaviski, T. Ye, B. Zheng, J. D. Simon and M. D. Edington, Time-resolved spectroscopic studies of radiationless decay processes in photoexcited hemocyanins, *J. Phys. Chem. B*, 2001, **105**, 1478–1483.

219 N. Saga, Y. Kimura, N. Hirota and M. Terazima, Photothermalization processes of charge transfer complexes in liquids studied by the transient grating method, *Chem. Phys. Lett.*, 2000, **332**, 496–502.

220 N. Saga, Y. Kimura, M. Terazima and N. Hirota, Energy dissipation process of photo-excited charge transfer complexes in fluids studied by the transient grating method, *Anal. Sci.*, 2001, **17**, S234–S236.

221 L. J. Rothberg, J. D. Simon, M. Bernstein and K. S. Peters, Pulsed laser photoacoustic calorimetry of metastable species, *J. Am. Chem. Soc.*, 1983, **105**, 3464–3468.

222 P. A. MacFaul, D. D. M. Wayner and K. U. Ingold, Measurement of N-H bond strengths in aromatic amines by photoacoustic calorimetry, *J. Org. Chem.*, 1997, **62**, 3413–3414.

223 L. J. J. Laarhoven, P. Mulder and D. D. M. Wayner, Determination of bond dissociation enthalpies in solution by photoacoustic calorimetry, *Acc. Chem. Res.*, 1999, **32**, 342–349.

224 M. S. Churio, K. P. Angermund and S. E. Braslavsky, Combination of laser-induced optoacoustic spectroscopy (LIOAS) and semiempirical calculations for the determination of molecular volume changes: the photoisomerization of carbocyanines, *J. Phys. Chem.*, 1994, **98**, 1776–1782.

225 M. A. Rodriguez and S. E. Braslavsky, Photoisomerization of azobenzenecarboxylic acids and their potassium salts: evidence of structural volume changes associated with hydrogen bond formation, *J. Phys. Chem. A*, 1999, **103**, 6295–6300.

226 A. Feis, B. Wegewijs, W. Gartner and S. E. Braslavsky, Role of the triplet state in retinal photoisomerization as studied by laser-induced optoacoustic spectroscopy, *J. Phys. Chem. B*, 1997, **101**, 7620–7627.

227 I. Michler, A. Feis, M. A. Rodriguez and S. E. Braslavsky, Structural volume changes upon photoisomerization: a laser-induced optoacoustic study with a water-soluble nitrostilbene, *J. Phys. Chem. A*, 2001, **105**, 4814–4821.

228 R. M. Williams, A. F. McDonagh and S. E. Braslavsky, Structural volume changes upon photoisomerization of the bilirubin-albumin complex: a laser-induced optoacoustic study, *Photochem. Photobiol.*, 1998, **68**, 433–437.

229 R. P. Herbrich and R. Schmidt, Investigation of the pyrene/N,N′-diethylaniline exciplex by photoacoustic calorimetry and fluorescence spectroscopy, *J. Photochem. Photobiol., A*, 2000, **133**, 149–158.

230 N. Haralampus Grynaviski, C. Ransom, T. Ye, M. Rozanowska, M. Wrona, T. Sarna and J. D. Simon, Photogeneration and quenching of reactive oxygen species by urocanic acid, *J. Am. Chem. Soc.*, 2002, **124**, 3461–3468.

231 K. M. Hanson and J. D. Simon, The origin of the wavelength-dependent photoreactivity of trans-urocanic acid, *Photochem. Photobiol.*, 1998, **67**, 538–540.

232 S. E. Forest and J. D. Simon, Wavelength-dependent photoacoustic calorimetry study of melanin, *Photochem. Photobiol.*, 1998, **68**, 296–298.

233 D. Wrobel, A. Planner, I. Hanyz, A. Wielgus and T. Sarna, Melanin-porphyrin interaction monitored by delayed luminescence and photoacoustics, *J. Photochem. Photobiol., B*, 1997, **41**, 45–52.

234 D. Wrobel, I. Hanyz, A. Planner, A. Dudkowiak and T. Sarna, Energy deactivation pathways of porphyrins and dopa melanin in polyvinyl alcohol systems, *J. Photochem. Photobiol., B*, 1998, **47**, 165–172.